Spatial, temporal and source contribution assessments of BC over the northern interior of South Africa

Kgaugelo Euphinia Chiloane[1], Johan Paul Beukes[1], Pieter Gideon van Zyl[1], Petra Maritz[1], Ville Vakkari[2], Miroslav Josipovic[1], Andrew Derick Venter[1], Kerneels Jaars[1], Petri Tiitta[1,3], Markku Kulmala[4], Alfred Wiedensohler[5], Catherine Liousse[6], Gabisile Vuyisile Mkhatshwa[7], Avishkar Ramandh[8], Lauri Laakso[1,2]

[1] {Unit for Environmental Sciences and Management, North-West University, Potchefstroom Campus, South Africa}

[2] {Finnish Meteorological Institute, Helsinki, Finland}

[3] {Department of Environmental and Biological Sciences, Univ. of Eastern Finland, P.O. Box 1627, 70211 Kuopio, Finland}

[4] {Department of Physics, University of Helsinki, Finland}

[5] {Leibniz Institute for Tropospheric Research, Leipzig, Germany}

[6] {Laboratoire d'Aérologie, Université Paul Sabatier-CNRS, OMP, 14 Avenue Edouard Belin, 31400 Toulouse, France}

[7] {Research, Testing and Development, Eskom SOC Ltd, Rosherville, South Africa}

[8] {Sasol Technology R&D (Pty) Limited, South Africa}

Correspondence to: J.P. Beukes (paul.beukes@nwu.ac.za)

Abstract

After carbon dioxide (CO_2), aerosol black carbon (BC) is considered to be the second most important contributor to global warming. Africa is one of the least studied continents, although it is regarded as the largest source region of atmospheric BC. Southern Africa is an important sub-source region, with savannah and grassland fires likely to contribute to elevated BC mass concentration levels. South Africa is the economic and industrial hub of southern Africa. To

Atmospheric
Chemistry
and Physics
Discussions

1   date, little BC mass concentration data have been presented for South Africa in the peer-

2   reviewed public domain. This paper presents equivalent black carbon (eBC) (derived from an

3   optical absorption method) data collected from three sites, where continuous measurements

4   have been conducted, i.e. Elandsfontein (EL), Welgegund (WG) and Marikana (MA), as well

5   elemental carbon (EC) (determined by evolved carbon method) at five sites where samples were

6   collected once a month on a filter and analysed off-line, i.e. Louis Trichardt (LT), Skukuza

7   (SK), Vaal Triangle (VT), Amersfoort (AM) and Botsalano (BS). All these sites are located in

8   the interior of South Africa.

9   Analyses of eBC and EC spatial mass concentration patterns across the eight sites indicate that

10   the mass concentrations in the South African interior are in general higher than what has been

11   reported for the developed world and that different sources are likely to influence different sites.

12   The mean eBC or EC mass concentrations for the background sites (WG, LT, SK, BS) and sites

13   influenced by industrial activities and/or nearby settlements (EL, MA, VT and AM) ranged

14   between 0.7 and 1.1, and 1.3 and 1.4 $\mu g/m^3$, respectively.

15   Similar seasonal patterns were observed at all three sites where continuous measurement data

16   were collected (EL, MA and WG), with the highest eBC mass concentrations measured during

17   June to October, indicating contributions from household combustion in the cold winter months

18   (June-August), as well as savannah and grassland fires during the dry season (May to mid-

19   October). Diurnal patterns of eBC at EL, MA and WG indicated maximum concentrations in

20   the early mornings and late evenings, and minima during daytime. From the patterns it could

21   be deduced that for MA and WG, household combustion and savannah, and grassland fires were

22   the most significant sources, respectively.

23   Possible contributing sources were explored in greater detail for EL, with five main sources

24   being identified as coal-fired power stations, pyrometallurgical smelters, traffic, household

25   combustion, as well as savannah and grassland fires. Industries on the Mpumalanga Highveld

26   are often blamed for all forms of pollution, due to the NO_2 hotspot over this area that is attributed

27   to NOx emissions from industries and vehicle emissions from the Johannesburg-Pretoria

28   megacity. However, a comparison of source strengths indicated that household combustion,

29   and savannah and grassland fires were the most significant sources of eBC, particularly during

30   winter and spring months, while coal-fired power stations, pyro-metallurgical smelters and

31   traffic contribute to eBC mass concentration levels year round.

Atmospheric
Chemistry
and Physics
Discussions

1 Introduction

Aerosol black carbon (BC) is the carbonaceous fraction of ambient particulate matter that absorbs incoming short-wave solar radiation and terrestrial long-wave radiation, which has a warming effect on the atmosphere (IPCC, 2013). Although BC has a relatively short atmospheric lifetime (days to weeks), it has significant regional effects on temperature, cloud amount and precipitation. Over snow-covered areas, the surface albedo can be significantly reduced due to the deposition of BC, and this may considerably influence the local and regional climate (Ramanathan and Carmichael, 2008; Jacobson, 2004). Direct observations of reduced albedo resulting from long-range-transported BC into Arctic areas were reported by Stohl et al. (2006). It was estimated that BC may have contributed to more than half of the observed Arctic warming since 1890, most of this occurring during the last three decades (Shindell and Faluvegi, 2008). After CO_2, BC is considered to be the second most important contributor to global warming (Bond et al., 2004; IPCC, 2013). According to some authors, reducing BC emissions may be the fastest means of slowing global warming in the near future. In addition to the afore-mentioned effects, BC is a major contributor to fine particulate matter in the atmosphere that can also have negative health effects (Hansen et al., 1984, Cachier, 1995; IPCC, 2013).

Atmospheric BC is a primary species (Putaud et al., 2004; Pöschl, 2005) that is emitted by combustion processes, particularly from fossil fuel combustion, diesel engine exhaust, as well as open biomass fires and household combustion (Cachier, 1995; Cooke and Wilson, 1996; Bond and Sun, 2004; IPCC, 2013). Globally, approximately 20% of BC is emitted from residential biofuel burning, 40% from fossil fuels and 40% from open biomass burning such as forest and savannah fires (Hansen et al., 1988; Cooke and Wilson, 1996; Wolf and Cachier, 1998; Pope, 2002;). BC from fossil fuels is estimated to contribute a global mean radiative forcing of 0.04 watts per square metre (W/m²) (IPCC, 2013).

There are large uncertainties associated with emissions of BC, its aging during atmospheric transportation and its removal by precipitation (Bond and Sun, 2004), which are reflected in uncertainties in the global effect of BC (e.g. Bond et al., 2013). Presently, the majority of aerosol radiative impact assessments are based on models (Bond et al., 2013; IPCC, 2013), both on local and global scales, which incorporate measured aerosol properties. However, this approach involves several assumptions, which could lead to significant uncertainties (Andreae and Gelencser, 2006; Masiello, 2004; Bond et al., 2013). For a better understanding of the

Atmospheric
Chemistry
and Physics
Discussions

1　transport, removal and climatic impacts of atmospheric BC, accurate and up-to-date

2　measurements covering large spatial areas and long temporal periods are required.

3　Africa is one of the least studied continents, although it is regarded as the largest source region

4　of atmospheric BC (Liousse et al., 1996; Kanakidou et al., 2005). Southern Africa is an

5　important sub-source region, with savannah and grassland fires (anthropogenic and natural)

6　being prevalent across this region, particularly during the dry season, when almost no

7　precipitation occurs (Formenti et al., 2003; Tummon et al., 2010; Laakso et al., 2012; Vakkari

8　et al., 2014; Mafusire et al., 2016). Studies by Swap et al. (2004) indicated that savannah and

9　grassland fire plumes from southern Africa affect Australia and South America. South Africa

10　is the economic and industrial hub of southern Africa with large anthropogenic point sources

11　(Lourens et al., 2011). However, the relative importance of BC contributions from these

12　anthropogenic sources in South Africa is still largely unknown and few BC-related papers have

13　been published in the peer-reviewed public domain. Venter et al. (2012) used BC mass

14　concentration data collected at the Marikana monitoring station to verify the origin of CO and

15　PM_{10}, but did not consider BC further. Collett et al. (2010) only presented a single diurnal plot

16　for BC mass concentration measured at the Elandsfontein monitoring station in 2010.

17　Hyvärinen et al. (2013) used BC mass concentration data collected at the Welgegund

18　monitoring station to illustrate the use of a newly developed method to correct BC mass

19　concentration values measured with a multi-angle absorption photometer (MAAP). In addition,

20　Martins (2009) determined elemental carbon (EC) and organic carbon (OC) mass

21　concentrations from three two-week winter campaigns and one two-week summer campaign at

22　two sites, as part of the framework of the Deposition of Biogeochemical Important Trace

23　Species (DEBITS)-International Global Atmospheric Chemistry (IGAC) in Africa project

24　(Galy-Lacaux et al., 2003; Martins et al., 2007). However, this data have not yet been published

25　in the peer-reviewed scientific domain. Maritz et al. (2015) and Aurela et al. (2016) presented

26　limited EC mass concentration data from some regional background sites in South Africa. Kuik

27　et al. (2015) used the Weather Research and Forecasting model, including chemistry and

28　aerosols (WRF-Chem), to analyse the contribution of anthropogenic emissions to the total

29　tropospheric BC mass concentrations from September to December 2010 in South Africa.

30　However, significant underestimations and uncertainties with regard to BC mass concentrations

31　were reported by the afore-mentioned authors.

32　From the above-mentioned, the need for improved BC mass concentration data for South Africa

Atmospheric
Chemistry
and Physics
Discussions

1 is evident. This paper presents spatial and temporal assessments of equivalent black carbon

2 (eBC) derived from an optical absorption method and elemental carbon (EC) determined by an

3 evolved carbon method (definitions according to Petzold et al., 2013) mass concentrations over

4 the northern interior of South Africa, as well as potential contributing sources of eBC at

5 Elandsfontein, a site located on the South African Highveld.

6 **2   Measurement locations and methods**

7 **2.1   Measurement sites**

8 In this paper, eBC or EC mass concentration data from eight measurement stations are

9 presented. At three of these stations, continuous high resolution eBC measurements were

10 conducted, i.e. Elandsfontein (EF), Welgegund (WG) and Marikana (MA), while at the

11 remaining five stations, i.e. Louis Trichardt (LT), Skukuza (SK), Vaal Triangle (VT),

12 Amersfoort (AF) and Botsalano (BS), samples were collected once a month on a filter for a

13 period of 24 hours and analysed off-line to yield EC. The locations of these sites within a

14 regional context are indicated in Figure 1. In order to contextualise all the sites, a brief

15 description of each site is presented below.

16   **Insert Figure 1**

17 *2.1.1 Elandsfontein*

18 The Elandsfontein monitoring station (26.25°S 29.42°E; 1750 m.a.m.s.l.) is located on the top

19 of a hill approximately 200 km east of Johannesburg in the highly industrialised South African

20 Highveld (Collett et al., 2010). The site is relatively frequently affected by plumes from coal-

21 fired power stations, metallurgical smelters and a large petrochemical operation that occur

22 within an approximately 60 km radius around the site (Laakso et al., 2012). The site was used

23 for the European Integrated Project on Cloud Climate, Aerosols and Air Quality Interactions

24 (EUCAARI) project for measurements outside Europe; with state-of-the-art instruments for

25 comprehensive aerosol measurements (Laakso et al., 2012; Kulmala et al., 2009).

26 Measurements were conducted from February 2009 to January 2011 with a PM_{10} inlet.

27 *2.1.2 Marikana*

28 The Marikana monitoring station (25.70°S 27.48°E; 1170 m.a.m.s.l.) is located in a small

29 village situated approximately 35 km east of the city of Rustenburg, in the North West Province

30 of South Africa. Within an approximately 55 km radius from this site there are 11

31 pyrometallurgical smelters and at least twice as many mines (feeding the afore-mentioned

32 smelters) (Venter et al., 2012). However, there were no mining and/or industrial activities

Atmospheric
Chemistry
and Physics
Discussions
Open Access
EGU

1   within a 1 km radius of the site. The closest surroundings included semi-formal (government-

2   built housing developments, mostly with some form of informal housing additions by the

3   occupants) and informal (self-erected, sometimes unauthorised, mostly without municipal

4   services) settlements, a formal residential area with a gas station and shops, as well as tarred

5   and untarred roads serving the communities in this area (Venter et al., 2011; Hirsikko et al.,

6   2012). Measurements were conducted from September 2008 to May 2010 with a PM_{10} inlet.

7   *2.1.3 Welgegund*

8   The Welgegund measurement station (www.welgegund.org, 26.57°S 26.94°E, 1480 m.a.m.s.l.)

9   is situated approximately 100 km west of Johannesburg on the property of a commercial farmer.

10   It is representative of a regional background site, but is also affected by aged plumes from major

11   source regions in South Africa (Jaars et al., 2014; Tiitta et al., 2014; Venter et al., 2016). A

12   detailed description of the Welgegund measurement station and related source regions was

13   relatively recently presented by Beukes et al. (2013). Measurements reported in this paper

14   covered the period June 2010 to May 2012, with either PM_{10} (1 June 2010 to 25 August 2010,

15   as well as 1 September 2011 to 31 May 2012) or PM_1 (26 August 2010 to 31 August 2011)

16   inlets being employed.

17   *2.1.4 DEBITS sites*

18   Maritz et al. (2015) introduced all the DEBITS sites for which data is presented. Therefore only

19   synopses of the site descriptions, taken from the afore-mentioned paper, are given here. The

20   DEBITS project is an international long-term project that mainly focuses on measuring

21   atmospheric deposition of pollutants (Galy-Lacaux *et al.,* 2003; Mphepya et al, 2004 and 2006;

22   Conradie et al., 2016). The Louis Trichardt (22.99 S 30.02 E; 1300 m.a.m.s.l.), Skukuza

23   (24.99 S 31.58 E; 267 m.a.m.s.l.), Vaal Triangle (26.72 S 27.88 E; 1320 m.a.m.s.l.),

24   Amersfoort (27.07 S 29.87 E; 1628 m.a.m.s.l.) and Botsalano (25.54 S 25.75 E;

25   1424 m.a.m.s.l.) sites were operated within the afore-mentioned programme. Amersfoort is

26   situated in a grassland biome and is affected by anthropogenic activities on the Mpumalanga

27   Highveld. Louis Trichardt is a rural site that is predominantly used for agricultural purposes

28   within the savannah biome. Skukuza is a regional background site within the savannah biome

29   and is situated in a protected area (Kruger National Park). The Vaal Triangle site is within the

30   grassland biome and is situated in a highly industrialised area, affected by emissions from

31   various industries, traffic and household combustion. Botsalano is a regional background site

32   that is situated within the savannah biome and a protected area (Botsalano Game Reserve). In

Atmospheric
Chemistry
and Physics
Discussions

1   this paper EC sampled at these sites with a PM$_{10}$ inlet was reported for the period March 2009

2   to April 2011.

3   **2.2   Sampling and analysis methods**

4   Aerosol BC mass concentration can be measured using both online and off-line methods. In

5   this paper eBC was measured with a light-absorption method and EC with a thermo-optical

6   method (Petzold et al., 2013).

7   *2.2.1   Online sampling and analysis of eBC*

8   eBC mass concentration was continuously measured at Elandsfontein, Marikana and

9   Welgegund with a Thermo Scientific, Model 5012 Multi-angle Absorption Photometer

10   (MAAP) with time resolutions of 1 minute that was converted to 15 minute averages. The

11   MAAP measures aerosol eBC with a filter-based method that uses a combination of reflection

12   and transmission measurements together with a radiative transfer model to yield eBC

13   concentration (Petzold and Schönlinner, 2004). However, if the automated filter change in

14   MAAP occurs at a high eBC concentration, an artefact may occur (Hyvärinen et al., 2013). In

15   this study, the MAAP eBC measurements were corrected for this artefact according to

16   Hyvärinen et al. (2013). Furthermore, the MAAPs at Welgegund and Elandsfontein were

17   operated at reduced flow rates, which decreased the number of such filter change artefacts.

18   *2.2.2 Off-line sampling and analysis of EC*

19   Twenty four (24)-hour PM$_{10}$ aerosol samples were collected on quartz filters (with a deposit

20   area of 12.56 cm^2) once a month at Louis Trichardt, Skukuza, Vaal Triangle, Amersfoort and

21   Botsalano for the entire measurement period reported. Sample preparation and analysis were

22   according to the methods described by Maritz et al. (2015). The quartz filters were prebaked at

23   900°C for four hours and cooled down in a desiccator, prior to sample collection. MiniVol

24   samplers developed by the United States Environmental Protection Agency (US-EPA) and the

25   Lane Regional Air Pollution Authority were used during sampling (Baldauf et al., 2001). In

26   this study, samples were collected at a flow rate of 5 L/min, which was verified by using a

27   handheld flow meter. Filters were handled with tweezers while wearing surgical gloves, as a

28   precautionary measure to prevent possible contamination of the filters. All thermally pre-

29   treated filters were also visually inspected to ensure that there were no weak spots or flaws.

30   After inspection, acceptable filters were weighed and packed in airtight Petri dish holders until

31   they were used for sampling. After sampling, the filters were again placed in Petri dish holders,

32   sealed off, bagged and stored in a portable refrigerator for transport to the laboratory. At the

Atmospheric
Chemistry
and Physics
Discussions

1   laboratory the sealed filters were stored in a conventional refrigerator. Twenty four hours prior

2   to analysis, samples were removed from the refrigerator and weighed prior to analysis. Several

3   methods can be used to analyse EC collected on filters (Chow et al., 2001). In this study, the

4   IMPROVE thermal/optical (TOR) protocol (Chow et al., 1993; Chow et al. 2004;

5   Environmental Analysis Facility, 2008; Guillaume et al., 2008) was applied using a Desert

6   Research Institute (DRI) analyser. With this method, the filters are subjected to volatilisation

7   at temperatures of 120, 250, 450 and 550°C in a pure helium (He) atmosphere and at

8   temperatures of 550, 700 and 800°C in a mixture of He (98%) and oxygen (O_2) (2%)

9   atmosphere. In this process, carbon compounds that are released are converted to CO_2 in an

10   oxidation furnace with a manganese dioxide (MnO_2) catalyst at 932°C. Then, the flow passed

11   through a digester where the CO_2 is reduced to methane (CH_4) on a nickel-catalysed reaction

12   surface. The amount of CH_4 formed is detected by a flame ionisation detector (FID), which is

13   converted to carbon mass using a calibration coefficient. The carbon mass peaks detected

14   correspond to the different temperatures at which the seven separate carbon fractions, which

15   include three elemental carbon (EC) fractions, were released. These fractions were depicted as

16   different peaks on the thermogram, of which the surface areas were proportional to the amount

17   of CH_4 detected. The DRI instrument can detect EC as low as 0.1 $\mu g/cm^2$.

18   **2.3   Savannah and grassland fire locations**

19   A number of products can be used to obtain savannah and grassland fire locations. Fire

20   locations presented in this paper were obtained from the remote sensing observations of fires

21   from the MODIS collection 5 burned area product (Roy et al., 2008; MODIS, 2014).

22   **2.4   Air mass back trajectory analysis**

23   The Hybrid Single-Particle Lagrangian Integrated Trajectory (HYSPLIT 2014) model (version

24   4.8), developed by the National Oceanic and Atmospheric Administration (NOAA) Air

25   Resources Laboratory (ARL) was used to calculate air mass histories (Draxler and Hess, 2004).

26   Meteorological data from the GDAS archive of the National Centre for Environmental

27   Prediction (NCEP) of the United States National Weather Service (USNWS) and archived by

28   the ARL (Air Resources Laboratory, 2014a), was used as input. This data has a 40 or 80 km

29   grid resolution, depending on the year considered (NASA, 2015), with all the data used in this

30   study having 40 km grid resolution. All trajectories were calculated for 24 hours backwards, to

31   arrive on the hour at an arrival height of 100 m above ground level. An arrival height of 100 m

32   was chosen, since the orography in HYSPLIT is not well defined, which could result in

Atmospheric
Chemistry
and Physics
Discussions

1 increased error margins on individual trajectory calculations if lower arrival heights are used

2 (Air Resources Laboratory, 2014c). For such calculated back trajectories, maximum error

3 margins of 15 to 30% of the trajectory distance travelled have been estimated (Stohl, 1998;

4 Riddle et al., 2006; Vakkari et al., 2011).

5 **2.5   Linking ground-based measurements with point sources using back trajectories**

6 This method was introduced by Maritz et al. (2015) who used it to link ambient organic carbon

7 (OC) and EC concentrations to potential sources. The same method was applied here, to assess

8 if large point sources and in- or semi-formal settlements contributed to ambient eBC

9 concentrations. The method relates eBC concentrations measured at a particular sampling site

10 with the closest distance between the hourly arriving trajectory and the afore-mentioned sources

11 (large point sources, as well as in- and semi-formal settlements). Figure 2 presents an

12 illustration of the method applied for a specific sampling site to determine the shortest distance

13 between a 24-hour back trajectory and large point sources. The distances between the large

14 point sources (indicated by the black markers) and a specific back trajectory were calculated

15 for each of the hourly locations of the 24-hour back trajectory (indicated by the red dots on

16 Figure 2). The red line indicates the shortest distance between hourly locations of this specific

17 trajectory and large point sources (i.e. petrochemical operations, coal-fired power stations and

18 pyro-metallurgical smelters). The weaknesses of the afore-mentioned method were that

19 downwind point sources and/or in- or semi-formal settlements, very close to the monitoring

20 site, could in some instances be the closest point source/in- or semi-formal settlements.

21 Additionally, dilution due to distance travelled by the trajectories was not considered.

22   **Insert Figure 2**

23 **2.6   Determining the relative contribution of eBC from sources**

24 In order to determine the relative strength of eBC mass concentration sources, detailed

25 correlation analyses were performed for eBC peaks. For instance, it is well known that plumes

26 from coal-fired power stations on the Mpumalanga Highveld are characterised by a

27 simultaneous increase in NO, NO_2 and SO_2 concentrations (Collect et al., 2010; Lourens et al.,

28 2011). Figure 3 shows the eBC, SO_2, NO_2, NO and H_2S data measured on 14 February 2009.

29 In this figure, it is evident that two well-defined coal-fired power plant plumes were observed

30 between 09:15 and 11:30 based on SO_2, NO_2 and NO time series, as well as between 18:00 and

31 21:00. However, both of these coal-fired power plant-associated plumes did not raise the

32 baseline eBC meaningfully. There was, however, a significant eBC plume between 02:00 and

9

Atmospheric
Chemistry
and Physics
Discussions

1   08:30, which coincided perfectly with a simultaneous increase in H_2S. This eBC plume was

2   therefore associated with the source that emitted the H_2S. For each such plume the excess eBC

3   (Δ eBC) was determined, with Δ eBC defined as the eBC concentration above the baseline, as

4   indicated in the top pane of Figure 3.

5   **Insert Figure 3**

6   **2.7   Multiple linear regression analysis**

7   Several techniques were applied in this paper to characterise possible sources of eBC mass

8   concentrations measured at the various stations, e.g. seasonal patterns, diurnal patterns, back

9   trajectory analyses, and identifying sources based on coincidental increases in species time

10   series. In an attempt to further critically evaluate deductions made from these methods, multiple

11   linear regression (MLR) analyses were conducted. Linear regression is denoted by constants

12   or known parameters (c), an independent variable (x) and a dependent variable (y) by fitting a

13   linear equation to the observed data. MLR is characterised by more than one independent

14   variable (x). In MLR, the relationship between the dependent variable (y) and independent

15   variables (x) is denoted by Equation 1.

16   $y = c_0 + c_1x_1 + c_2x_2 + c_3x_3 + \dots\dots\dots\dots c_zx_z$ Eq. 1

17   In this study, MLR was used to determine an equation for the dependent variable eBC. MLR

18   was used to determine the optimum combination of independent variables to derive an equation

19   that could be used to predict eBC concentrations. Root mean square error (RMSE) was used to

20   compare the calculated values with the measured values. Several authors have previously

21   applied similar methods for various atmospheric species (e.g. Awang et al., 2015; Du Preez et

22   al., 2015; Venter et al., 2015).

23   **3   Results and discussions**

24   **3.1   Spatial variation**

25   In Figure 4, a box and whisker plot indicating the statistical eBC or EC mass concentrations for

26   each of the sites is presented. The significant difference in number of samples (N) is due to the

27   fact that at the DEBITS sites EC mass concentrations were only measured once per month over

28   a 24-sampling period, whereas at the other sites, one-minute eBC data were collected that were

29   converted to 15 min averages.

30   **Insert Figure 4**

31   Of all the sites considered, the highest mass concentrations were measured at VT that had a

Atmospheric
Chemistry
and Physics
Discussions

1   median EC of 3.2 µg/m^3 and a mean of 4.4 µg/m^3 for the entire measurement period. Although

2   sources will be considered in greater detail later, the higher EC mass concentration levels at VT

3   can be attributed to various possible sources. Firstly, this area is densely populated with large

4   semi-formal and informal settlements. This indicates that household combustion for space

5   heating and cooking could be a significant source of EC. Secondly, the area experience

6   relatively higher traffic volumes and several large point sources (including petrochemical and

7   related chemical industries, two coal-fired power stations and numerous metallurgical smelters)

8   occur in the area. Thirdly, the site experiences less dilution of due to the close proximity of the

9   sources to the measurement site that contribute to the observed elevated levels of EC mass

10   concentration.

11   The eBC at Elandsfontein, as well as the EC at Marikana and Amersfoort sites indicated similar

12   levels with median and mean values of 0.8 and 1.3, 1.2 and 1.7, and 1.1 and 1.4 µg/m^3

13   respectively. Elandsfontein and Amersfoort lie within the well-known NO_2 hotspot over the

14   Mpumalanga Highveld identified from satellite observations (Lourens et al., 2012) and are

15   therefore likely to be influenced by industrial activities in this area. Marikana can be affected

16   by household combustion from in- and semi-formal settlements that are located close to the

17   measurement site, as well as the large pyrometallurgical sources occurring in the area (Venter

18   et al., 2012; Hirsikko et al., 2012).

19   The background sites, i.e. Welgegund, Botsalano, Louis Trichardt and Skukuza had lower eBC

20   or EC levels compared to other locations, with median and mean concentrations of 0.4 and 0.7,

21   0.7 and 0.9, 0.8 and 0.9, and 0.9 and 1.1 µg/m^3, respectively. All these background sites are

22   likely to be affected most by regional savannah and grassland fires that are common in southern

23   Africa or by pollutants transported from other parts of the country. However, Welgegund,

24   which is the furthest west of these sites, is likely to be affected less by savannah and grassland

25   fires due to the dryer biomes, i.e. the Kalahari and Karoo that are located to the west of this site.

26   These drier biome regions produce less biomass that can burn (Mafusire et al., 2016). It is

27   therefore understandable that Welgegund had lower eBC levels than the other background sites.

28   Obviously, Elandsfontein, Marikana, Vaal Triangle and Amersfoort will also be affected by

29   regional savannah and grassland fires, in addition to the possible sources already mentioned.

30   The eBC and EC concentrations presented for all the sites considered (Figure 4) should also be

31   contextualised. The background site with the lowest PM_{10} eBC concentrations reported here,

32   i.e. Welgegund, had similar or higher eBC mass concentration values than typical western

Atmospheric
Chemistry
and Physics
Discussions

1   European background sites. BC mass concentrations of less than 0.2 to 0.3 µg/m^3 have been

2   reported for western parts of northern Europe (e.g. Yttri et al., 2007). At natural and rural

3   European background sites, values of 0.3 to 0.5 and 0.6 to 1.6 µg/m^3 have been reported,

4   respectively (e.g. Putaud et al., 2004; Hyvärinen et al., 2011). The other South African

5   background sites reported here, i.e. Botsalano, Louis Trichardt and Skukuza, had higher mean

6   and median values than the afore-mentioned European background/natural sites. The

7   industrial/urban/household affected sites reported here, i.e. Elandsfontein, Marikana, Vaal

8   Triangle and Amersfoort had higher average eBC or EC mass concentration levels than, for

9   instance, an urban site in a large European city, where BC mass concentrations had an average

10 of approximately 1.0 µg/m^3 (Järvi et al., 2008; Viidanoja et al., 2002). In general, it can

11 therefore be stated that eBC or EC mass concentrations across the measurement area considered

12 are relatively high.

13 Apart from the spatial information and possible indication of contributing sources obtained

14 from Figure 4, it is also evident from the comparison of the PM$_1$ and PM$_{10}$ eBC data of

15 Welgegund that most of the eBC resides in the PM$_1$ size fraction.

16 **3.2   Temporal variations**

17 **3.2.1   Seasonal variations**

18 In order to determine seasonal patterns, only the site where continuous measurements were

19 conducted was considered. Monthly statistical distributions of eBC mass concentrations for

20 Elandsfontein, Welgegund and Marikana measurement sites are presented in Figure 5. As is

21 evident from these figures, there is a distinct and similar seasonal pattern observed at all three

22 sites, with the highest eBC mass concentrations measured in June to October. These months

23 coincide with the colder winter months of June to August, as well as the dry season on the South

24 African Highveld occurring between May and middle October. Venter et al. (2012) previously

25 indicated that household combustion for cooking and space heating in informal and semi-formal

26 settlements during winter could be a significant eBC mass concentration source on a local scale.

27 However, it has not yet been determined whether such household combustion could also make

28 a significant regional contribution in South Africa. During the dry season, increased savannah

29 and grassland wild fires occur, which contributed to increased atmospheric eBC concentrations

30 (Bond et al., 2004, Saha and Despiau, 2009). The influence of both of these potential eBC

31 sources, i.e. household combustion and wild fires, will be discussed later in Section 3.3.

32   **Insert Figure 5**

3.2.2 Diurnal variations

Average diurnal plots as well as average seasonal diurnal plots (separate for summer, autumn, winter and spring) for the stations where continuous eBC mass concentration data were gathered, i.e. Elandsfontein, Marikana and Welgegund (both PM_1 and PM_{10}), are presented in Figure 6.

Insert Figure 6

The Elandsfontein diurnal plot indicates that the main source of eBC is not high stack emissions. eBC would have peaked after 11:00, as has been indicated for NO_2 by Collet et al. (2010) if eBC originated mainly from industrial high stack emissions. The area in which Elandsfontein is situated, is a well-known international NO_2 hotspot, with tropospheric column densities similar to what is observed over south-east Asia (Lourens et al., 2012). It is widely accepted that NO_2 in this hotspot mainly originates from coal-fired power stations. Therefore, if eBC mainly originated from these large point sources, eBC concentrations would also have peaked, similar to NO_2, after the breakdown of the night-time inversion layers. Additionally, the winter diurnal plot for Elandsfontein indicates substantially higher values during night-time when the planetary boundary layer (PBL) is less well mixed, which re-enforces the notion that the major origin of eBC is from low-level sources, rather than industrial high stacks that were designed to have effective stack heights above the low level inversion layer heights. At this site the daily evolution of the PBL starts approximately three to four hours after sunrise (varies between 05:07 and 06:56 local time), which results in increasing atmospheric mixing down from the upper atmosphere including high stack emissions (Korhonen et al., 2014). Therefore, the likely eBC sources during winter (June to August) and the dry season (May to middle October) can be attributed to household combustion, as well as savannah and grassland fires, respectively, not industrial high stack emissions. The industries on the Mpumalanga Highveld are often blamed for all forms of pollution, due to the NO_2 hotspot over this area that is attributed to NOx emissions from industries and vehicle emissions from the Johannesburg-Pretoria megacity (Lourens et al., 2012; Lourens et al., 2016).

In contrast to Elandsfontein, eBC concentrations at Marikana peaked in the early mornings (05:00-09:00) and again in the early to late evenings (17:30-22:00). These times correlate with the peak times for household combustion for space heating and cooking in the nearby in- and semi-formal settlements (Venter et al. 2012). Seasonal timing of the peak eBC concentration in the diurnal plots confirms that household combustion is the main source at this site. In winter,

Atmospheric
Chemistry
and Physics
Discussions

1   during which time daylight hours are shorter, the peak morning eBC concentration is at ~07:00

2   and the evening peak at ~18:00; whereas, during summer, with longer daylight hours, the peak

3   morning eBC concentration is at ~06:00 and the evening peak at ~20:00. During the cold winter

4   months, space heating is a priority, apart from cooking, while in summer, household combustion

5   would mainly be used for cooking. These seasonal household combustion use patterns are

6   reflected by the diurnal eBC patterns for Marikana.

7   The eBC diurnal plots of Welgegund do not indicate well-defined peaks as observed for

8   Marikana. This is expected, since there are no semi- or informal settlements located close to

9   the Welgegund station. Additionally, there are also no large point sources close to Welgegund,

10   as there are at Elandsfontein. Therefore, only sources that have a regional influence are likely

11   to affect eBC levels at Welgegund. It is therefore likely that savannah and grassland fires,

12   especially in the winter and early spring, are mainly responsible for eBC levels measured at

13   Welgegund and mainly long-range transportation during the wet season. The lower PBL during

14   the evenings and early mornings will concentrate the eBC and contribute to eBC levels rising

15   in the evening and only decreasing three to four hours after sunrise, as suggested by Korhonen

16   et al. (2014). This effect is strongest in the winter months.

17   **3.3   eBC source identification**

18   *3.2.1 General*

19   As has already been indicated, there are various possible sources for eBC, e.g. industrial,

20   household combustion, traffic, and savannah and grassland fires. In this section, possible

21   significant contributing sources are considered further. Figure 7 indicates the fire pixel counts

22   calculated from MODIS (collection of 5 burned area product) (Roy et al., 2008) within the

23   entire southern Africa (10-35˚S and 10-41˚E) indicated on the primary y-axis, as well as fire

24   pixel counts within a radius of 125 km around measurement sites where high resolution EBD

25   data was gathered on the secondary y-axis.

26   **Insert Figure 7**

27   It is important to note that it is difficult to separate the influence of various sources at a specific

28   site, since the measured eBC originates from a mixture of contributing sources. Therefore,

29   Figure 7 was considered first, since it provided guidance about which periods would be best to

30   consider for the different sources. For instance, there are very few savannah and grassland fires

31   during December to February every year in the northern interior of South Africa. The savannah

32   and grassland fires that do occur during this period occur in the southern Western Cape, which

14

1   will not influence eBC levels in the northern interior significantly. In addition, minimal

2   household combustion takes place in December to February, since it is the warmest months.

3   Considering the afore-mentioned, it is best to isolate industrial and traffic related eBC sources

4   during December to February.

5   It is clear for the overall southern African fire frequencies, as well as those around each site

6   (Figure 7) that August and September have the highest savannah and grassland fire intensities.

7   This is the driest period, just before the onset of the first rains, usually in middle October. We

8   can therefore isolate savannah and grassland fires best in this period, since its effect is strongest.

9   The influence of household combustion is also not that strong in this period; since it is already

10 becoming warmer and therefore less space heating is required. By considering aerosol particle

11 concentrations at Marikana, Vakkari et al. (2013) proved that the evening peak associated with

12 household combustion was significantly lower in September than in June to July.

13 Since it is coldest in June and July, the effect of household combustion for space heating is at

14 its strongest, making the isolation of the household combustion effect better during these

15 months.

16 In the following sections, eBC contributions from the above-mentioned sources, i.e. industrial,

17 traffic, savannah and grassland fires, and household combustion, will be explored in greater

18 detail for the Elandsfontein site only. This site was chosen, since it can be affected by all the

19 afore-mentioned sources, while the other sites where continuous high resolution data were

20 gathered will mainly be influenced by savannah and grassland fires (Welgegund) or household

21 combustion (Marikana).

22 *3.3.2   Industrial contribution to eBC at Elandsfontein*

23 Numerous large industrial point sources linked to coal utilisation occur in the South African

24 interior, e.g. coal-fired power stations that produce most of South Africa's electricity, large

25 petrochemical operations utilising coal gasification and numerous pyro-metallurgical smelters

26 utilising coal and coal-related products as carbonaceous reductants for the production of various

27 steels and alloys (Collet et al., 2010; Lourens et al., 2011; Beukes et al., 2012). Previously, it

28 has been indicated that some of these large point sources contribute significantly to certain

29 pollutant concentrations, e.g. the NO_2 hotspot observed with satellite observations over the

30 Highveld, mainly due to coal-fired power stations that do not de-SO_x or de-NO_x and traffic

31 emissions (Lourens et al., 2012). However, the possible contributions of these large point

32 sources to atmospheric BC concentrations have not yet been investigated for South Africa.

1   As previously indicated, Elandsfontein is situated within the well-known NO_2 hotspot, with

2   various large points sources located in close proximity (Collet et al., 2010; Lourens et al., 2011).

3   The diurnal eBC concentration plots of Elandsfontein (Figure 6) indicated that it is unlikely that

4   industrial high stack emissions were the main source of eBC at this site. However, this

5   postulation has to be proven. In Figure 8, eBC concentrations measured at Elandsfontein were

6   plotted against the shortest distances that back trajectories passed any large point source, during

7   the summer months (December to February), when minimal household combustion, as well as

8   savannah and grassland fires occur. Although there was no clear correlation (Figure 8), the

9   results indicated that at least some trajectories passing closer to these large industrial point

10   sources had higher eBC concentrations. This suggests that eBC contributions from large

11   industrial point sources cannot be ignored, notwithstanding the diurnal patterns, indicating that

12   high stack industrial emissions were not the main source (Figure 6).

13   **Insert Figure 8**

14   In order to quantify the relative contribution of large point sources at Elandsfontein, eBC peaks

15   that coincided with peaks of other pollutants, which are characteristic of large point sources in

16   that area, were considered for the December to February period. Two distinct types of

17   contributing sources were identified, i.e. eBC peaks that coincided with SO_2, NO_2 and NO, as

18   well as eBC peaks that only coincided with H_2S. From literature, it is known that plumes from

19   coal-fired power plants on the South African Highveld are characterised by coincidental SO_2,

20   NO_2 and NO increases (Collet et al., 2010; Lourens et al., 2011). Although it is not shown here,

21   eBC plumes that were associated with these species were confirmed to have originated from

22   coal-fired power stations with back trajectory analyses. However, H_2S peaks that coincided

23   with the eBC peaks could have been from various sources, e.g. the large petrochemical plant

24   near Secunda, pyro-metallurgical smelters in the area or smouldering coal dumps that burn as a

25   result of spontaneous combustion. In order to identify the origin of the eBC peaks that were

26   associated with H_2S only, a map on which all back trajectories that arrived at Elandsfontein

27   during these eBC peaks were plotted, is presented in Figure 9, together with a wind rose for

28   such events. From these figures, it is evident that the back trajectories that were associated with

29   simultaneous eBC and H_2S concentration peaks only passed over the sector between the

30   northwest and northeast from Elandsfontein. This is the area where all the pyro-metallurgical

31   smelters are located. Smouldering coal dumps occur in all directions from Elandsfontein.

32   Additionally, no trajectories associated with coincidental eBC and H_2S increases had passed

Atmospheric
Chemistry
and Physics
Discussions

Open Access

1   over the petrochemical operation. It therefore seems likely that the eBC contribution associated

2   with H_2S originates from the pyro-metallurgical smelters in the sector located between

3   northwest and northeast from Elandsfontein.

4   **Insert Figure 9**

5   *3.3.3   Traffic contribution to eBC at Elandsfontein*

6   From literature, it seems feasible to associate increased BC concentrations with traffic

7   emissions, particularly diesel-powered vehicles (Cachier, 1995; Cooke and Wilson, 1996; Bond

8   and Sun, 2005). The Mpumalanga Highveld around Elandsfontein is the area where most

9   thermal coal is mined in South Africa, which is mostly transported by diesel trucks via various

10   roads criss-crossing the area as indicated in Figure 10a. However, the closest tarred road, i.e.

11   the R35, passes Elandsfontein approximately 4.7 km to the east. This road is also one of the

12   most utilised for coal road transportation. Additionally, to the north of Elandsfontein, numerous

13   such tarred roads are located, e.g. the national N12 and N4 highways pass Elandsfontein

14   approximately 38 km to the north and north-west. It therefore seems reasonable that the traffic-

15   related eBC back trajectory map (Figure 10a) is somewhat biased toward the east and north,

16   although limited contributions from other sectors are also evident. The wind rose showing the

17   prevailing wind direction during periods when eBC plumes that coincided with NO_2 plumes

18   were observed (Figure 10b) also indicates the sources to be mainly from the east, i.e. where the

19   R35 passes Elandsfontein.

20   **Insert Figure 10**

21

22   *3.3.4   Household combustion contribution to eBC at Elandsfontein*

23   Venter et al. (2012) indicated that household combustion for space heating and cooking in in-

24   and semi-formal settlements contributes significantly to poor air quality in such settlements. In

25   Figure 11, the relationships between monthly average and median eBC, against monthly mean

26   and median temperatures for Elandsfontein, are presented. As is evident from the results

27   presented in Figure 11, there is a significant correlation between eBC concentration and

28   temperature, if August and September are ignored (indicated with hollow markers in Figure

29   11). During these months, significant eBC contributions can be expected from savannah and

30   grassland fires (see Figure 7). The correlation between eBC concentration and temperature

31   indicates that household combustion for space heating contributes significantly to eBC levels

32   measured at Elandsfontein, especially during the colder months when household combustion is

Atmospheric
Chemistry
and Physics
Discussions

1   used more frequently for space heating.

2   **Insert Figure 11**

3   Similar to what was done for large industrial point sources (Figure 8), eBC concentrations were

4   drawn as a function of the closest distance that back trajectories had passed in- and semi-formal

5   settlement for Elandsfontein. However, this was done only for the winter months of June and

6   July for both years, since household combustion contributions could then be better isolated from

7   savannah and grassland fire contributions during these periods. These results are presented in

8   Figure 12. Although not conclusive, the results presented indicate that, in general, higher eBC

9   concentrations were observed when trajectories passed closer to in- and semi-formal settlements

10   in June and July.

11   **Insert Figure 12**

12   Household combustion could result in the emission of various atmospheric species (Venter et

13   al., 2012). However, to be able to determine the Δ eBC for household combustion at

14   Elandsfontein, atmospheric species that simultaneously increased with eBC had to be identified.

15   Experimentally, it was found that simultaneous increases in NO_2, SO_2 and H_2S, but not NO

16   characterised household plumes measured at Elandsfontein. Low-grade coal that is burned in

17   ineffective stoves is commonly for household combustion in the Mpumalanga Highveld, due to

18   such coal being relative inexpensive. The use thereof results in NO_x, SO_2 and H_2S emissions.

19   During the cold winter months of June and July, strong inversion layers trap pollutants emitted

20   closer to ground level and prevent the mixing and subsequent transportation thereof. The low-

21   level emissions from in- and semi-formal settlements are therefore not dispersed before the

22   inversion layers break up in mid-morning. A previous study have indicated that the PBL starts

23   growing around 10:00 local time at Elandsfontein during the winter months (Korhonen et al.,

24   2014). It can therefore be accepted that the low-level inversion layers also start dissipating at

25   that time. The long residence time of air masses around in- and semi-formal settlements in

26   winter before being dispersed, as well as additional transport time, results in NO being oxidised

27   to NO_2 prior to these plumes being measured at Elandsfontein.

28   Figure 13a indicates back trajectories associated with household combustion contribution to

29   eBC levels. Most of these back trajectories passed over the Thubelihle and Kriel settlements,

30   which are located 12.4 and 13.8 km from Elandsfontein, respectively. Apart from this relatively

31   local eBC influence from household combustion, most trajectories associated with household

32   combustion eBC plumes passed over the sector between east and north-north-east, where the

Atmospheric
Chemistry
and Physics
Discussions

1   cities of Witbank and Middelburg, as well as the Johannesburg-Pretoria mega-city are located.

2   These larger cities have many more large in- and semi-formal settlements associated with them

3   than the smaller towns in the area do. The wind rose showing the prevailing wind direction

4   during periods when eBC plumes that coincided with NO_2, SO_2 and H_2S plumes were observed

5   (Figure 13b) also indicates the sources to be mainly from more or less the same direction as

6   most of the back trajectories.

7   **Insert Figure 13**

8   *3.3.5   Savannah and grassland fire contribution to eBC at Elandsfontein*

9   Vakkari et al. (2014) relatively recently indicated how savannah and grassland fire emission

10   aerosols are changed via atmospheric oxidation in South Africa. To positively identify

11   savannah and grassland fire plumes, the afore-mentioned authors used CO and eBC as

12   coincidental increasing species. However, CO was not measured at Elandsfontein and therefore

13   the positive identification of savannah and grassland plume could not be undertaken using this

14   method. Additionally, the plumes of savannah and grassland fires occurring in neighbouring

15   countries arriving at Elandsfontein will be diluted and aged. Such regional fires lift the entire

16   eBC baseline, rather than exhibiting well-defined plumes that can be separated from the baseline

17   (Mafusire et al., 2016), as was done for the industrial, traffic and household combustion sources.

18   Thus far in the paper, we have considered August and September as the months in which

19   savannah and grassland fires frequencies peak. However, some household combustion might

20   still occur in August. Therefore, to determine the overall baseline increase as a result of

21   savannah and grassland fires, only September was considered as being representative of

22   savannah and grassland fires, while the summer months (December to February) can be

23   considered as the baseline. By subtracting the September eBC mean from the summer mean,

24   the eBC baseline increased by 2.01 $\mu g/m^3$. This increase will be contextualised with the

25   previously investigated sources in the next section.

26   *3.3.6   Contextualisation of eBC source strengths at Elandsfontein*

27   Up to now, the individual eBC sources for Elandsfontein were discussed, but their strengths

28   were not compared with one another. In Figure 14, the comparison of the Δ eBC from coal-

29   fired power stations, pyro-metallurgical smelters, traffic, household combustion, as well as

30   savannah and grassland fires for Elandsfontein is presented. The relative savannah and

31   grassland fire source strength is not statistically presented with a box and whisker as for the

32   other sources, but only with a black star that indicates the mean eBC baseline increase during

Atmospheric
Chemistry
and Physics
Discussions

1   September if compared to the summer months of December to February. The data presented in

2   Figure 14 were normalised to account for variations in PBL height at Elandsfontein. This was

3   done by using the monthly average PBL daily maximum heights reported by Korhonen et al.

4   (2014) for 2010 at Elandsfontein. Unfortunately no such data existed for 2009, therefore the

5   2009 monthly PBL heights were assumed to be similar to 2010. Thereafter the ratios of the

6   average PBL daily maximum heights for each of the periods during which certain sources could

7   be better isolated (i.e. December to February for large point sources and traffic emission; June

8   to July to household combustion) were calculated, compared to the average PBL daily

9   maximum heights for August and September (period with peak savannah and grassland fire

10   occurrence). The Δ eBC for each of the sources identified in the December to February, as well

11   as June to July periods where then adjusted with these ratios to account for variations in the

12   PBL, which could have a significant dilution or concentration effect on the measured eBC

13   values, from which the Δ eBCs were derived. The results indicate the significant source strength

14   of household combustion, as well as savannah and grassland fires, as measured at Elandsfontein.

15   However, coal-fired power stations, pyro-metallurgical and/or char plants and traffic contribute

16   year round, while household combustion, as well as savannah and grassland fires only

17   contribute significantly in May to August, and June to September, respectively. Bond et al.

18   (2013) indicated relatively high BC emissions from biofuel cooking (calculated for Africa in

19   total), but did not indicate space heating to contribute significantly. However, our data seem to

20   prove that space heating does contribute meaningfully to eBC levels in South Africa during the

21   colder winter months (June-July).

22   **Insert Figure 14**

23   Vakkari et al (2014) used Δ eBC in relation to other species to characterise differences in plumes

24   of savannah and grassland fires. In a similar manner, these ratios for Δ eBC divided by other

25   species reported in this paper were determined and are presented in Figure 15. The median

26   and/or mean values indicated in this figure could be used in subsequent modelling studies to

27   quantify eBC if only the emissions of other species are known.

28   **Insert Figure 15**

29   **3.4   Mathematical confirmation of eBC sources at Elandsfontein**

30   Four scenarios were investigated with MLR analyses. Firstly, MLR analysis was conducted for

31   the entire monitoring period at Elandsfontein. As is evident from the top left pane in Figure 16,

32   the RMSE difference between the actual measured eBC concentration and the calculated eBC

Atmospheric
Chemistry
and Physics
Discussions

1   concentrations if only one independent parameter was included in the optimum MLR solution

2   was approximately 1.54.   The RMSE difference could be reduced by including more

3   independent parameters in the optimum MLR solution.   However, it was found that the

4   inclusion of more than nine independent parameters did not further reduce the RMSE difference

5   significantly.

6   **Insert Figure 16**

7   From the MLR analysis conducted for the entire measurement period at Elandsfontein, the

8   actual MLR equation could be obtained, which is presented as Equation 2. With this equation,

9   eBC at Elandsfontein could be calculated. The comparisons between actual and calculated

10   (with Equation 2) eBC concentrations are presented in Figure 17. From this comparison, it is

11   evident that Equation 2 could be used to predict eBC at Elandsfontein relatively accurately.

12   $y=$ -33.7038 + (0.0050 x O_3) + (0.0387 x SO_2) + (0.0006 x NO_2) + (0.0722 x H_2S) + (-0.0174

13   x RH) + (0.0997 x WS) + (0.0005 x WD) + (0.0421 x P) + (2.27433 x T-grad)   Eq. 2

14   **Insert Figure 17**

15   In order to use MLR to verify whether the eBC contribution sources were identified correctly

16   in Section 3.3, MRL analyses were also conducted for the different time periods defined for

17   isolation of the various sources, i.e. December to February for industrial and traffic sources,

18   June and July for household combustion, and August and September for savannah and grassland

19   fires.

20   As is indicated in Equation 3 and the top right pane of Figure 16, the optimum MLR solution

21   obtained for the December to February period included seven independent variables in the

22   equation. Firstly, the fact that fewer independent variables were required to reduce the RMSE

23   optimally, if compared with the overall period (top left pane of Figure 16), indicates that the

24   December to February period is influenced by fewer sources. Secondly, the identity of the

25   independent variables and the sign (positive or negative) associated with them in Equation 3

26   are noteworthy. Increased O_3 concentrations led to lower eBC, which indicates that aged air

27   masses had lower eBC than fresh plumes do. This supports the notion that relatively nearby

28   industry and traffic sources dominate. The increased eBC, associated with increased NO_2 and

29   H_2S concentrations in Equation 3, supports the identity of the specific source types previously

30   identified, i.e. coal-fired power stations, pyrometallurgical smelters, as well as traffic emissions.

31   The remaining independent variables in Equation 3 are associated with meteorological

Atmospheric
Chemistry
and Physics
Discussions

1   parameters, which could indicate that meteorological patterns (e.g. atmospheric stability as

2   indicated by T-gradient) could have a significant influence on plumes containing eBC measured

3   at Elandsfontein.

4    $y = -30.3494 + (-0.0170 \times O_3) + (0.0002 \times NO_2) + (0.1005 \times H_2S) + (0.1350 \times T) +$

5        $(0.0102 \times RH) + (0.0338 \times P) + (1.8185 \times \text{T-gradient})$ Eq. 3

6   For the June and July periods, Equation 4 and the lower left pane of Figure 16 indicate that the

7   optimum MLR solution included only four independent variables in the equation. This low

8   number of independent variables confirm that this time period was dominated by a much less

9   complicated source mixture than the overall time period. During June to July, it was previously

10   indicated that household combustion dominated eBC contributions, which is confirmed by the

11   SO_2- and NO_2-associated eBC increases indicated by Equation 4. As stated earlier, the

12   household combustion plumes measured at Elandsfontein are likely to be NO depleted, due to

13   the stagnant nature of air masses during the evening and early morning that result in the

14   oxidation of NO to NO_2. This phenomenon is also indicated by Equation 3. Lastly, increased

15   RH will be associated with increased moisture-induced particle growth that could result in

16   quicker aerosol deposition and therefore reduced eBC levels.

17   $y = 1.7061 + (0.0453 \times SO_2) + (-0.1059 \times NO) + (0.0855 \times NO_2) + (-0.0191 \times RH)$ Eq. 4

18   For the August and September periods, Equation 5 and the lower right pane of Figure 16

19   indicate that the optimum MLR solution included eight independent variables in the equation.

20   Although not as low as for the June and July period, this low number of independent variables

21   confirms that the August and September periods were less complicated than the overall time

22   period. According to Equation 5, increased O_3 for August to September had a positive constant

23   associated with it, which indicates that aged savannah and grassland fire plumes increase the

24   eBC concentrations, while the NO_2 and SO_2 positive constant associations and the negative NO

25   constant association indicate that household combustion still makes contributions during this

26   time. This makes sense, since August is still regarded as a winter month with significant

27   household combustion for space heating taking place. However, since the August and

28   September periods already include warmer spring months (September for both years) with

29   lower household combustion, the H_2S, T, RH and T-grad relationships observed in summer also

30   already make a meaningful contribution.

31   $y = -2.549 + (0.0511 \times O_3) + (0.0316 \times SO_2) + (-0.5737 \times NO) + (0.1840 \times NO_2) +$

32       $(0.0433 \times H_2S) + (0.0469 \times T) + (0.0145 \times RH) + (2.4877 \times \text{T-grad})$ Eq. 5

4   Conclusions

This paper presents the most comprehensive eBC spatial and temporal, as well as source contribution assessments for the South African interior that has been published in the peer-reviewed public domain to date. Limited EC data was also presented, which expanded the overall spatial extent covered in the paper.

Analyses of eBC and EC spatial concentration patterns at eight sites indicate that concentrations in the South African interior are in general higher than what has been reported for the developed world, e.g. Western Europe. The highest levels were observed at Vaal Triangle, which were attributed to EC emissions from household combustion emanating from in- and semi-formal settlements, as well as traffic and large points sources. eBC or EC levels at Elandsfontein, Amerfoort and Marikana were similar, but likely originated from different sources. Elandsfontein and Amersfoort lie within the well-known NO_2 hotspot over the Mpumalanga Highveld and are therefore likely to be influenced by industrial activities in this area, while Marikana is in close proximity to in- and semi-formal settlements. The background sites, i.e. Welgegund, Botsalano, Louis Trichardt and Skukuza had lower eBC or EC levels. All these background sites are likely to be affected most by regional savannah and grassland fires, which are common in southern Africa.

Similar seasonal patterns were observed at all three sites where high resolution eBC data were collected, i.e. Elandsfontein, Marikana and Welgegund, with the highest eBC concentrations measured in June to October. These months coincide with the cold winter months of June to August that indicate possible contributions from household combustion, as well as the dry season on the South African Highveld occurring between May and mid-October, which indicates contributions from savannah and grassland fires.

Diurnal patterns indicated that at Elandsfontein industrial high stack emissions were not the most significant source, since no peaks were observed after the breakup of lower-level inversion layers. The diurnal patterns at Marikana revealed household combustion for space heating and cooking to be the most significant sources. At Welgegund, the most significant source contributions were most likely regional savannah and grassland fires.

Possible contributing eBC sources were explored in greater detail for Elandsfontein only. Industrial sources could be isolated best during the summer months of December to February, since very few savannah and grassland fires, as well as household combustion for space heating occur then. Coincidental plumes of SO_2, NO_2, NO and eBC were used to identify plumes from

Atmospheric
Chemistry
and Physics
Discussions

1   coal-fired power stations, while coincidental increases of H_2S and eBC characterised eBC

2   contributions from pyrometallurgical smelters. During summer, coincidental increases of NO_2

3   and eBC were used to identify traffic emissions. The contribution of household combustion

4   was isolated during the coldest winter months of June and July. Coincidental increases of NO_2,

5   SO_2 and H_2S, with eBC, which did not correlate to NO increases, were found to characterise

6   household combustion plumes. Back trajectory analyses and wind roses supported the validity

7   of all the aforementioned source associations. Savannah and grassland fire plumes could not

8   be isolated since CO was not measured at Elandsfontein. However, the general baseline

9   increase in eBC levels between September (the peak fire frequency period) and the summer

10   months (with virtually no savannah and grassland fires) could be calculated and attributed to

11   savannah and grassland fire eBC emissions. At Elandsfontein, the eBC concentration in

12   September was comparable to the eBC concentration in June to July, which indicates that at this

13   location domestic heating and regional scale savannah and grassland fires are equally significant

14   sources of eBC. Furthermore, MLR analyses supported the seasonality of eBC sources at

15   Elandsfontein.

16   Although the source strengths of coal-fired power stations, pyro-metallurgical smelters and

17   traffic emissions were lower than that of household combustion, as well as savannah and

18   grassland fires, the first mentioned sources contribute year round, while the latter only

19   contributed significantly in May to August, and June to September, respectively. Of the fresh

20   industrial plumes, the highest eBC concentrations were associated with pyro-metallurgical

21   smelters. This is a very significant finding, since coal-fired power stations and petrochemical

22   operations have in the past been blamed for most of the pollution problems on the Mpumalanga

23   Highveld (mainly due to the NO_2 hotspot over this area). Therefore, pyrometallurgical sources

24   in this area need to be considered in greater detail in future studies.

25   Lastly, the calculated emission ratios of eBC and gaseous species that were presented could be

26   used in future studies to assess the eBC emission inventories for industrial and domestic sources

27   in South Africa.

28   **5   Acknowledgements**

Atmospheric
Chemistry
and Physics

Open Access

EGU

Discussions

Atmospheric
Chemistry
and Physics
Discussions

Open Access

6 References

Andreae, M.O., and Gelencser, A.: Black carbon or brown carbon? The nature of light absorbing carbonaceous aerosols. Atmospheric Chemistry and Physics, 6, 3131-3148, doi:10.5194/acp-6-3131-2006, 2006.

Andrews, E., Massoli, P., Hallar, A.G., Sedlacek, A., Freedman, A., Ogren, J.A., and Sheridan, P.: Absorption closure-filter-based absorption instruments compared to extinction-scattering measurements. Poster presentation at the European Aerosol Conference, Grenada, Spain, September, 2012.

Aurela, M., Beukes, J.P., Vakkari, V., Van Zyl, P.G., Teinilä, K., Saarikoski S. and Laakso L.: The composition of ambient and fresh biomass burning aerosols at a savannah site, South African Journal of Science, 112(5/6), Art. #2015-0223, 8 pages, doi: 10.17159/ sajs.2016/20150223, 2016.

Awang, N.R., Ramli, N.Y., Ahmad, S., and Elbayoumi, M.: Multivariate methods to predict ground level ozone during daytime, nighttime, and critical conversion time in urban areas. Atmospheric Pollution Research, 6, 726-734. Atmospheric Environment 43, 3918-3924, doi: 10.5094/APR.2015.081, 2015.

Baldauf, R.W., Lane, D.D., Marotz, G.A., and Wiener, R.W.: Performance evaluation of the portable MiniVOL particulate matter sampler. Atmospheric Environment, 35, 6087-6091, doi:10.1016/S1352-2310(01)00403-4, 2001.

Chow, J.C., Watson, J.G., Crow, D., Lowenthal, D.H., & Merrifield, T.: Comparison of IMPROVE and NIOSH carbon measurements. Aerosol Science and Technology, 34, 23-24, 2001.

Beukes, J.P., Vakkari, V., Van Zyl, P.G., Venter, A.D., Josipovic, M., Jaars, K., Tiita, P., Siebert, S., Pienaar, J.J., Kulmala, M., and Laakso, L.: Welgegund: long-term land atmosphere measurement platform in South Africa. iLeaps Newsletter, 12, 24-25, 2013.

Beukes, J.P., Vakkari, V., Van Zyl, P.G., Venter, A.D., Josipovic, M., Jaars, K., Tiitta, P., Kulmala, M., Worsnop, D., Pienaar, J.J., Virkkula, A. and Laakso, L.: Source region plume characterisation of the interior of South Africa as observed at Welgegund, Clean Air Journal, 23(1), 7-10, 2013.

Bond, T., Streets, D.G., Yarber, K.F., Nelson, S.M., Woo, J-H. and Klimont, Z.: A technology-based global inventory of black and organic carbon emissions from combustion. Journal of Geophysical Research, 109, doi:10.1029/2003JD003697, 2004.

Bond, T.C.: Can warming particles enter global climate discussions? Environmental Research

1   Letters 2 (October-December 2007), 045030, doi:10.1088/1748-9326/2/4/045030, 2007.

2   Bond, T.C., Doherty, S.J., Fahey, D.W., Forster, P.M., Berntsen, T., DeAngelo, B.J., Flanner,

3   M.G., Ghan, S., Kärcher, B., Koch, D., Kinne, S., Kondo, Y., Quinn, P., Sarofim, M.C.,

4   Schultz, M.G., Schulz, M., Venkataraman, C., Zhang, H., Zhang, S., Bellouin, N.,

5   Guttikunda, S.K., Hopke, P.K., Jacobson, M.Z.,. Kaiser, J.W., Klimont, Z., Lohmann, U.,

6   Schwarz, J.P., Shindell, D., Storelvmo, T., Warren, S.G., and Zender, C.S.: Bounding the

7   role of black carbon in the climate system: A scientific assessment. Journal of Geophysical

8   Research: Atmospheres, 118, 5380-5552, doi:10.1002/jgrd.50171, 2013.

9   Cachier, H., Auglagnier, F., Sarda, R., Gautier, F., Masclet, P., Besombes, J.-L., Marchand, N.,

10 Despiau, S., Croci, D., Mallet, M., Laj, P., Marinoni, A., Deveau, P.-A., Roger, J.-C., Putaud,

11 J.-P., Van Dingenen, R., Dell'Acqua, A., Viidanoja, J., Martins-Dos Santos, S., Liousse, C.,

12 Cousin, F., Rosset, R. Gardrat, E., and Galy-Lacaux, C.: Aerosol studies during the

13 ESCOMPTE experiment: An overview. Atmospheric Research, 74, 547-563,

14 doi:10.1016/j.atmosres.2004.06.013, 2005.

15 Chow, J.C., Watson, J.G., Pritchett, L.C., Pierson, W.R., Frazier, C.A., and Purcell, R.G.: The

16 DRI thermal/optical reflectance carbon analysis system: description, evaluation and

17 applications in U.S. Air quality studies. Atmospheric Environment, 27, 1185-1201,

18 doi:10.1016/0960-1686(93)90245-T, 1993.

19 Chow, J.C., Watson, J.G., Kuhns, H., Etyemezian, V., Lowenthal, D.H., Crow, D., Kohl, S.D.,

20 Engelbrecht, J.P., and Green, M.C.: Source profiles for industrial, mobile, and area sources

21 in the Big Bend Regional Aerosol Visibility and Observational study. Chemosphere, 54,

22 185-208, doi:10.1016/j.chemosphere.2003.07.004, 2004.

23 Collett, K, Piketh, S. and Ross, K: An assessment of the atmospheric nitrogen budget on the

24 South African Highveld, South African Journal of Science, 106,

25 doi:10.4102/sajs.v106i5/6.220, 2010.

26 Conradie, E.H., Van Zyl, P.G., Pienaar, J.J., Beukes, J.P., Galy-Lacaux, C., Venter, A.D., and

27 Mkhatshwa, G.V.: The chemical composition and fluxes of atmospheric wet deposition at

28 four sites in South Africa, accepted in Atmospheric Environment, doi:

29 10.1016/j.atmosenv.2016.07.033, 2016.

30 Cooke, W.F., and Wilson, J.N.: A global black carbon aerosol model. Journal of Geophysical

31 Research 101D, 19395-19408, doi:10.1029/96JD00671, 1996.

32 Draxler, R. R., and Hess, G. D.: Description of the HYSPLIT 4 Modelling System, NOAA

33 Technical Memorandum ERL ARL-224, 2004.

Atmospheric
Chemistry
and Physics
Discussions

Open Access

EGU

1   Environmental Analysis Facility (EAF). DRI Standard operating procedure.   86p.
2   Laboratoired'Aérologie – UMR 5560. http://www.aero.obs-mip.fr/spip.php?article489.
3   Accessed 16 June 2016, 2008.

4   Formenti, P., Elbert, W., Maenhaut, W., Haywood, J., Osborne, S., and Andreae, M.O.:
5   Inorganic and carbonaceous aerosols during the Southern African Regional Science
6   Initiative (SAFARI 2000) experiment: Chemical characteristics, physical properties, and
7   emission data for smoke from African biomass burning.   Journal of Geophysical Research,
8   108(D13), 8488, doi:10.1029/2002JD002408, 2003.

9   Guillame, B., Liousse, C., Galy-Lacaux, C., Rosset, R., Gardrat, E., Cachier, H., Bessagnet, B.,
10   and Poisson, N.: Modeling exceptional high concentrations of carbonaceous aerosols
11   observed at Pic du Midi in spring-summer 2003: Comparison with Sonnblick and Puy de
12   Dôme.   Atmospheric Environment, 42, 5140-5149, doi:10.1016/j.atmosenv.2008.02.024,
13   2008.

14 Hansen, A.D.A., Rosen, H. and Novakov, T.: The Aethalometer: an instrument for real-time
15   measurement of optical absorption by aerosol particles, The Science of the Total
16   Environment, 36, 191-196, doi:10.1016/0048-9697(84)90265-1, 1984.

17 Hirsikko, A., Vakkari, V., Tiitta, P., Manninen, H.E., Gagné, S., Laakso, H., Kulmala, M.,
18   Mirme, A., Mirme, S., Mabaso, D., Beukes, J.P. and Laakso, L.: Characterisation of sub-
19   micron particle number concentrations and formation events in the western Bushveld
20   Igneous Complex, South Africa,   Atmospheric Chemistry and Physics, 12, 3951–3967,
21   doi:10.5194/acp-12-3951-2012, 2012.

22 Hyvärinen, A.-P., Vakkari, V., Laakso, L., Hooda, R.K., Sharma, V.P., Panwar, T.S., Beukes,
23   J.P., Van Zyl, P.G., Josipovic, M., Garland, R.M., Andreae, M.O., Pöschl, U., and Petzold,
24   A.: Correction for a measurement artifact of the Multi-Angle Absorption Photometer
25   (MAAP) at high black carbon mass concentration levels. Atmospheric Measurement
26   Techniques, 6, 81-90, doi:10.5194/amt-6-81-2013, 2013.

27 HYSPLIT   User's   Guide-Version   4.   Last   revised: April   2013.
28   http://www.arl.noaa.gov/documents/reports/hysplit_user_guide.pdf. Accessed 13 February
29   2014.

30 Galy-Lacaux, C., Al Ourabi, H., Lacaux, J.-P., Pont, V., Galloway, J., Mphepya, J., Pienaar, K.,
31   Sigha, L., and Yoboué, V.: Dry and wet atmospheric nitrogen deposition in Africa. IGAC
32   Newsletter, January 2003, Issue no. 27, 6-11, 2003.

33 IPCC: Changes in atmospheric constituents and in radiative forcing, in climate change 2007:

Atmospheric
Chemistry
and Physics
Discussions

Open Access

EGU

1   The Physical Science Basis. Contribution of Working Group I to the Fourth Assessment

2   Report of the Intergovernmental Panel on Climate Change, 129, 132; available at

3   http://www.ipcc.ch/ipccreports/ar4-wg1.htm, accessed: 18 November 2011, 2007.

4   IPCC: Summary for Policymakers. In: Climate Change 2013: The Physical Science Basis.

5   Contribution of Working Group I to the Fifth Assessment Report of the Intergovernmental

6   Panel on Climate Change [Stocker, T.F., D. Qin, G.K. Plattner, M. Tignor, S.K. Allen, J.

7   Boschung, A. Nauels, Y. Xia, V. Bex and P.M. Midgley (eds.)]. Cambridge University Press,

8   Cambridge, United Kingdom and New York, NY, USA.

9   Jaars, K., Beukes, J.P., Van Zyl, P.G., Venter, A.D., Josipovic, M., Pienaar, J.J., Vakkari, V.,

10   Aaltonen, H., Laakso, H., Kulmala, M., Tiitta, P., Guenther, A., Hellén, H., Laakso. L., and

11   Hakola, H.: Ambient aromatic hydrocarbon measurements at Welgegund, South Africa.

12   Atmospheric Chemistry and Physics, 14, 4189-4227, doi:10.5194/acpd-14-4189-2014,

13   2014.

14   Jacobson, M., 2004. Climate response of fossil fuel and biofuel soot, accounting for soot's

15   feedback to snow and sea ice albedo and emissivity, 109 Journal of Geophysical Research:

16   Atmospheres, 109, D21201, doi:10.1029/2004JD004945, 2004.

17   Kanakidou, M., Seinfeld, J.H., Pandis, S.N., Barnes, I., Dentener, F.J., Facchini, M.C., Van

18   Dingenen, R., Ervens, B., Nenes, A., Nielson, C.J., Swietlicki, E., Putaud, J.P., Balkanski,

19   Y., Fuzzi, S., Horth, J., Moortgat, G.K., Winterhalter, R., Myhre, C.E.L., Tsigaridis, K.,

20   Vignati, E., Stephanou, E.G., and Wilson, J.: Organic aerosol and global climate modelling:

21   a review. Atmospheric chemistry and Physics, 5, 1053-1123, doi:1680-7324/acp/2005-5-

22   1053, 2005.

23   Kuik, F., Lauer, A., Beukes, J.P., Van Zyl, P.G., Josipovic, M., Vakkari, V., Laakso, L. and

24   Feig, G.T.: The anthropogenic contribution to atmospheric black carbon concentrations in

25   southern Africa: a WRF-Chem modeling study, Atmospheric Chemistry and Physics, 15,

26   8809–8830, doi: 10.5194/acp-15-8809-2015, 2015.

27   Kulmala, M., Asmi, A., Lappalainen, H., Carslaw, K. S., Pöschl, U., Baltensperger, U., Hov,

28   Ø., Brenguier, J.-L., Pandis, S. N., Facchini, M. C., Hansson, H.-C., Wiedensohler, A., and

29   O'Dowd, C.D.:. Introduction: European Integrated Project on Aerosol Cloud Climate and

30   Air Quality interactions (EUCAARI). Integrating aerosol research from nano to global

31   scales, Atmospheric Chemistry and Physics 9, 2825-2841, 2009.

32   Laakso, L., Vakkari, V., Virkkula, A., Laakso, H., Backman, J., Kulmala, M., Beukes, J.P., van

33   Zyl, P.G., Tiitta, P., Josipovic, M., Pienaar, J.J., Chiloane, K., Gilardoni, S., Vignati, E.,

Atmospheric
Chemistry
and Physics
Discussions

Open Access

EGU

1   Wiedensohler, A., Tuch, T., Birmili, W., Piketh, S., Collett, K., Fourie, G.D., Komppula,

2   M., Lihavainen, H., de Leeuw, G., and Kerminen, V.-M.: South African EUCAARI

3   measurements: seasonal variation of trace gases and aerosol optical properties. Atmospheric

4   Chemistry and Physics, 12, 1847-1864, doi:10.5194/acp-12-1847-2012, 2012.

5   Liousse, C., Penner, J.E., Chuang, C., Walton, J.J., Eddleman, H., and Cachier, H.: A global

6   three-dimensional model study of carbonaceous aerosols. Journal of Geophysical Research,

7   105, 26871-26890, 1996.

8   Lourens, A.S., Beukes, J.P., and Van Zyl, P.G.: Spatial and temporal assessment of gaseous

9   pollutants in the Highveld of South Africa. South African Journal of Science, 107(1/2), Art.

10   #269, 8 pages, doi: 10.4102/sajs.v107i1/2.269, 2011.

11   Lourens, A.S.M., Butler, T.M., Beukes, J.P., Van Zyl, P.G. Pienaar, J.J., Lawrence, M.G.:

12   Investigating photochemical processes in the Johannesburg-Pretoria megacity using a box

13   model, South African Journal of Science, 112(1/2), Art. #2015-0169, 11 pages,

14   doi: 10.17159/sajs.2016/2015-0169, 2016.

15   Mafusire, G., Annegarn, H.J., Vakkari, V., Beukes, J.P., Josipovic, M., Van Zyl, P.G. and

16   Laakso, L.: Submicrometer aerosols and excess CO as tracers for biomass burning air mass

17   transport over southern Africa, Journal of Geophysical Research – Atmopsheres, 121,

18   10262–10282, doi:10.1002/2015JD023965, 2016.

19   Martins, J.J., Dhammapala, R.S., Lachmann, G., Galy-Lacaux, C., & Pienaar, J.J.: Long-term

20   measurements of sulphur dioxide, nitrogen dioxide, ammonia, nitric acid and ozone in

21   southern Africa using passive samplers. South African Journal of Science, 103, 336-342.

22   2007.

23   Martins, J.J.: Concentrations and deposition of atmospheric species at regional sites in southern

24   Africa. MSc thesis NWU Potchefstroom, 224p. 2009.

25   Masiello, C.A.: New directions in black carbon organic geochemistry. Marine Chemistry 92,

26   201-213, doi:10.1016/j.marchem.2004.06.043, 2004.

27   MODIS: Obtaining   and   processing   MODIS   data.

28   http://www.yale.edu/ceo/Documentation/MODIS_data.pdf.

29   Mokdad, Ali H.: Actual Causes of Death in the United States, 2000. Journal of American

30   Medical Association, 291 (10), 1238-1245, 2004.

31   Mphepya, J.N., Pienaar, J.J., Galy-Lacaux, C., Held, G., and Turner, C.R.: Precipitation

32   Chemistry in Semi-Arid Areas of Southern Africa: A Case Study of a Rural and an Industrial

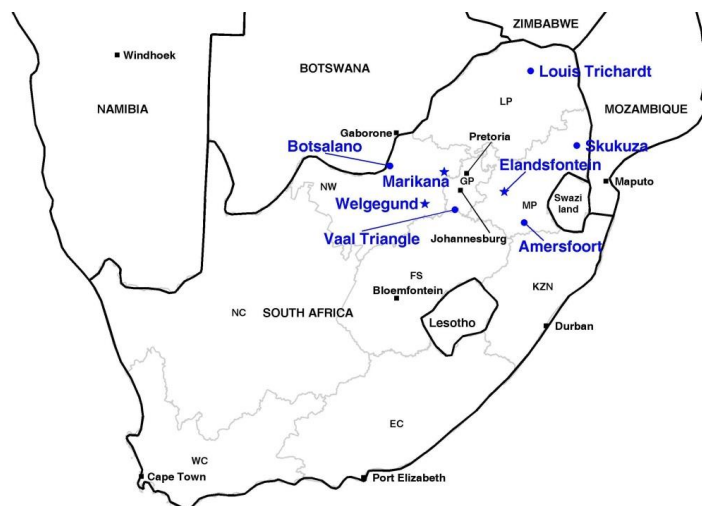33   Site.   Journal   of   Atmospheric   Chemistry,   47,   1-24,

Atmospheric
Chemistry
and Physics
Discussions

doi:10.1023/B:JOCH.0000012240.09119.c4, 2004.

Maritz, P., Beukes, J.P., Van Zyl, P.G. Conradie, E.H., Liousse, C., Galy-Lacau, C., Castéra, P., Ramandh, A., Mkhatshwa, G., Venter, A.D. and Pienaar, J.J.: Spatial and temporal assessment of organic and black carbon at four sites in the interior of South Africa, Clean Air Journal, 25(1), 20-33, doi: 10.17159/2410-972X/2015/v25n1a1, 2015.

Petzold, A., and Schönlinner, M.: Multi-angle absorption photometry: a new method for the measurement of aerosol light absorption and atmospheric black carbon. Journal of Aerosol Science 35, 421-441, doi:10.1016/j.jaerosci.2003.09.005, 2004.

Petzold, A., Ogren, J. A., Fiebig, M., Laj, P., Li, S.-M., Baltensperger, U., Holzer-Popp, T., Kinne, S., Pappalardo, G., Sugimoto, N., Wehrli, C., Wiedensohler, A., and Zhang, X.-Y.: Recommendations for reporting "black carbon" measurements, Atmospheric Chemistry and Physics, 13, 8365–8379, doi: 10.5194/acp-13-8365-2013, 2013.

Pope, C.A., Burnett, R.T., Thun, M.J., Calle, E.E., Krewski, D., Ito, K., and Thurston, G.D.: Lung cancer, cardiopulmonary mortality, and long-term exposure to fine particulate air pollution. Journal of the American Medical Association, 287 (9), 1132–1141, 2002.

Pöschl, U.: Atmospheric Aerosols: Composition, Transformation, Climate and Health Effects. Atmospheric Chemistry: Reviews. Angewandte Chemie International Edition, 44, 7520-7540, doi:10.1002/anie.200501122, 2005.

Putaud, J.-P., Raes, F., Van Dingenen, R., Brüggemann, E., Facchini, M.-C., Decesari, S., Fuzzi, S., Gehrig, R., Hüglin, C., Laj, P., Lorbeer, G., Maenhaut, W., Mihalopoulos, N., Müller, K., Querol, X., Rodriguez, S., Schneider, J., Spindler, G., ten Brink, H., Tørseth, K., and Wiedensohler, A.: A European aerosol phenomenology e 2: chemical characteristics of particulate matter at kerbside, urban, rural and background sites in Europe. Atmospheric Environment, 38, 2579-2595, doi:10.1016/j.atmosenv.2004.01.041, 2004.

Ramanathan, V., and Carmichael, G.: Global and regional climate changes due to black carbon. Nature Geoscience 1, 221-227, doi:10.1038/ngeo156, 2008.

Roy, D.P., Boschetti, L., Justice, C.O., and Ju, J.: The collection 5 MODIS burned area product: Global evaluation by comparison with the MODIS active fire product. Remote Sensing of Environment, 112, 3690-3707p. doi: 10.1016/j.rse.2008.05.013, 2008.

Saha A., and Despiau S.: Seasonal and diurnal variations of black carbon aerosols over a Mediterranean coastal zone. Atmospheric Research, 92, 27-41, doi:10.1016/j.atmosres.2008.07.007, 2009

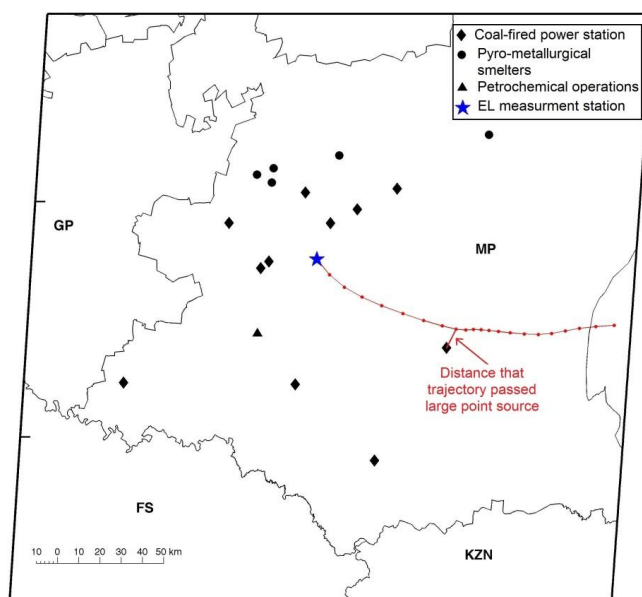Scholes, R.J., Ward, D.E. and Justice, C.O.: Emissions of trace gases and aerosol particles due

1 to vegetation burning in southern hemisphere Africa. Journal of Geophysical Research,
2 101(D19): 23,677-23,682, 1996.

3 Shindell, D.T., Levy II, H., Schwarzkopf, M.D., Horowitz, L.W., Lamarque, J.-F., and
4 Faluvegi, G.: Multimodel projections of climate change from short-lived emissions due to
5 human activities. Journal of Geophysical Research – Atmospheres, 113, D11109.
6 doi:10.1029/2007JD009152, 2008.

7 Stohl, A.: Computation, accuracy and application of trajectories – a review and bibliography.
8 Atmospheric Environment, 32(6), 947-966, doi: 10.1016/S1352-2310(97)00457-3, 1998.

9 Swap, R.J., Aranibar, J.N., Dowty, P.R., Gilhooly (III), W.P., and Macko, S.A.: Natural
10 abundance of ^{13}C and ^{15}N in C$_3$ and C$_4$ vegetation of southern Africa: patterns and
11 implications. Global Change Biology, 10, 350-358, doi:10.1046/j.1529-8817.2003.00702.x,
12 2004.

13 Swap, R.J., Annegarn, H.J., Suttles, J.T., King, M.D., Platnick, S., Privette, J.L., and Scholes
14 R.J.: Africa burning: A thematic analysis of the Southern African Regional Science Initiative
15 (SAFARI 2000), Journal of Geophysical Research, 108, 8465, doi:10.1029/2003JD003747,
16 2003.

17 Tummon, F., Solmon, F., Liousse, C., and Tadross, M.: Simulation of the direct and semidirect
18 aerosol effects on the southern Africa regional climate during the biomass burning season.
19 Journal of Geophysical Research D: Atmospheres, 115(19).   Art. no. D19206,
20 doi:10.1029/2009JD013738, 2010.

21 Tiitta, P., Vakkari, V., Croteau, P., Beukes, J.P., Van Zyl, P.G., Josipovic, M., Venter, A.D.,
22 Jaars, K., Pienaar, J.J., Ng, N.L., Canagaratna, M.R., Jayne, J.T., Kerminen, V.-M., Kokkola,
23 H., Kulmala, M., Laaksonen, A., Worsnop, D.R., and Laakso, L.: Chemical composition,
24 main sources and temporal variability of PM1 aerosols in southern African grassland.
25 Atmospheric Chemistry and Physics, 14, 1909–1927, doi: 10.5194/acp-14-1909-2014, 2014.

26 Venter, A.D., Vakkari, V., Beukes, J.P., Van Zyl, P.G., Laakso, H., Mabaso, D., Tiitta, P.,
27 Josipovic, M., Kulmala, M., Pienaar, J.J., and Laakso, L. An air quality assessment in the
28 industrialised western Bushveld Igneous Complex, South Africa. South African Journal of
29 Science, 108(9/10), Art. #1059, 10 pages, doi: 10.4102/sajs.v108i9/10.1059, 2012

30 Venter, A.D., Beukes, J.P., van Zyl, P.G., Brunke, E.G., Labuschagne, C., Slemr, F., Ebinghaus,
31 R., and Kock, H.: Statistical exploration of gaseous elemental mercury (GEM) measured at
32 Cape Point from 2007 to 2011. Atmospheric Chemistry and Physics, 15, 10271-10280,
33 doi: 10.5194/acp-15-10271-2015, 2015.

Atmospheric
Chemistry
and Physics
Discussions

Open Access

EGU

1   Venter, A.D., Beukes, J.P., Van Zyl, P.G., Josipovic, M., Jaars, K. and Vakkari, V.: Regional

2   atmospheric Cr(VI) pollution from the Bushveld Complex, South Africa. Atmospheric

3   Pollution Research, 7, 762–767, doi: 10.1016/j.apr.2016.03.009, 2016.

4   Viidanoja, J., Sillanpää, M., Laakia, J., Kerminen, V.-M., Hillamo, R., Aarnio, P., and

5   Koskentalo, T.: Organic and black carbon in $PM_{2.5}$ and PM_{10}: 1 year of data from an urban

6   site in Helsinki, Finland. Atmospheric Environment, 36, 3183-3193, doi:10.1016/S1352-

7   2310(02)00205-4, 2002.

8   Yttri, K.E., Aas, W., Bjerke, A., Cape, J.N., Cavalli, F., Ceburnis, D., Dye, C., Emblico, L.,

9   Facchini, M.C., Forster, C., Hanssen, J.E., Hansson, H.C., Jennings, S.G., Maenhaut, W.,

10   and Putaud, J.P., Torseth, K.: Elemental and organic carbon in PM10: a one year

11   measurement campaign within the European Monitoring and Evaluation Program EMEP.

12   Atmospheric Chemistry and Physics, 7, 5711-5725, 2007.

13   Wolf, E.W., and Cachier, H.: Concentrations and seasonal cycle of black carbon in aerosol at a

14   coastal Antarctic station. Journal of Geophysical Research, 103D, 11033-11041, 1998.
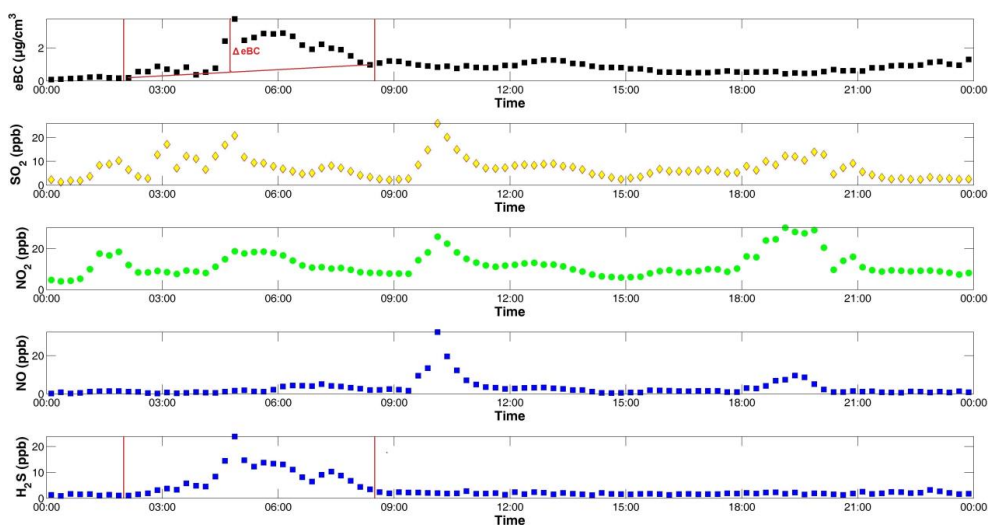
15

1

2   Figure 1.   Locations of the Elandsfontein (EF), Welgegund (WG), Marikana (MA), Louis
3   Trichardt (LT), Skukuza (SK), Vaal Triangle (VT), Amersfoort (AF) and Botsalano
4   (BS) measurement stations within a regional context. The sites where continuous
5   high resolution data were gathered are indicated with blue stars, while the sites
6   where filters were gathered and analysed off-line are indicated with blue dots.
7   Neighbouring countries, some major cities and South African provincial borders are
8   also indicated for additional regional contextualisation (Provinces: WC = Western
9   Cape; EC = Eastern Cape; NC = Northern Cape; FS = Free State; KZN = KwaZulu-
10   Natal; NW = North West; GP = Gauteng; MP = Mpumalanga and LP = Limpopo).

Atmospheric
Chemistry
and Physics
Discussions

1

Figure 2.   Example to illustrate the method applied to determine the shortest distance that each 24-hour back trajectory passed large point sources and/or in- or semi-formal settlements.
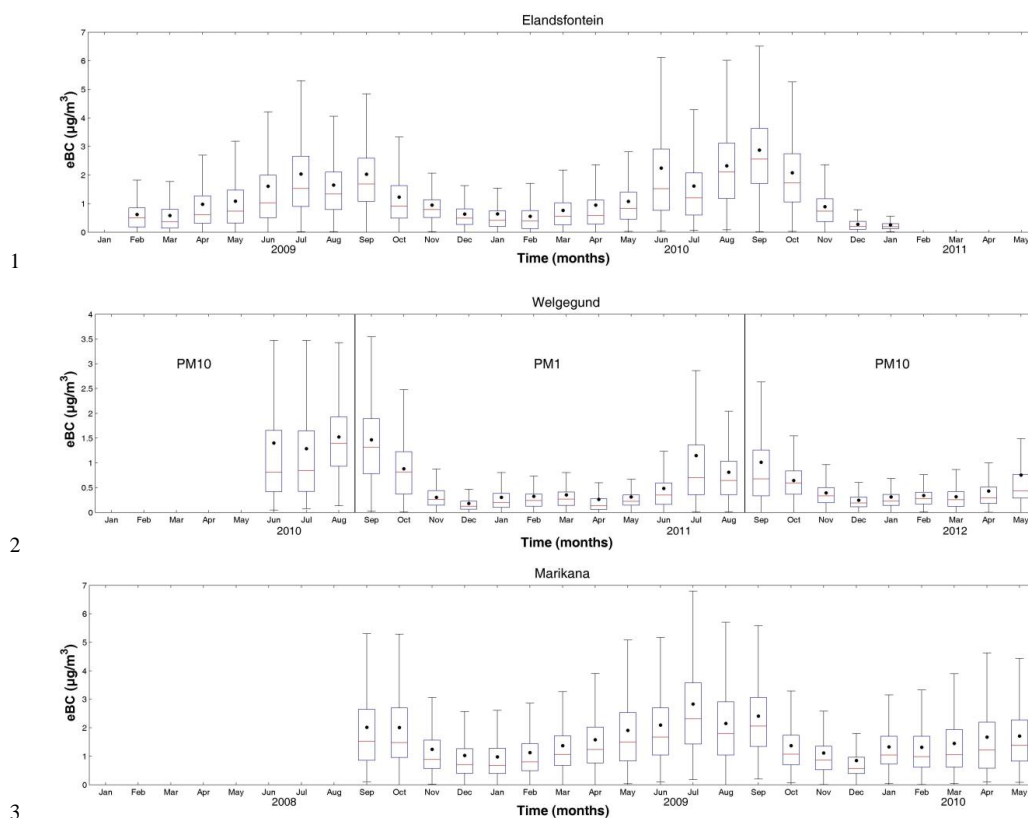
1

2 Figure 3. Example to illustrate how species were correlated with eBC in order to separate

3 sources from one another. The excess eBC (Δ eBC), defined as the eBC

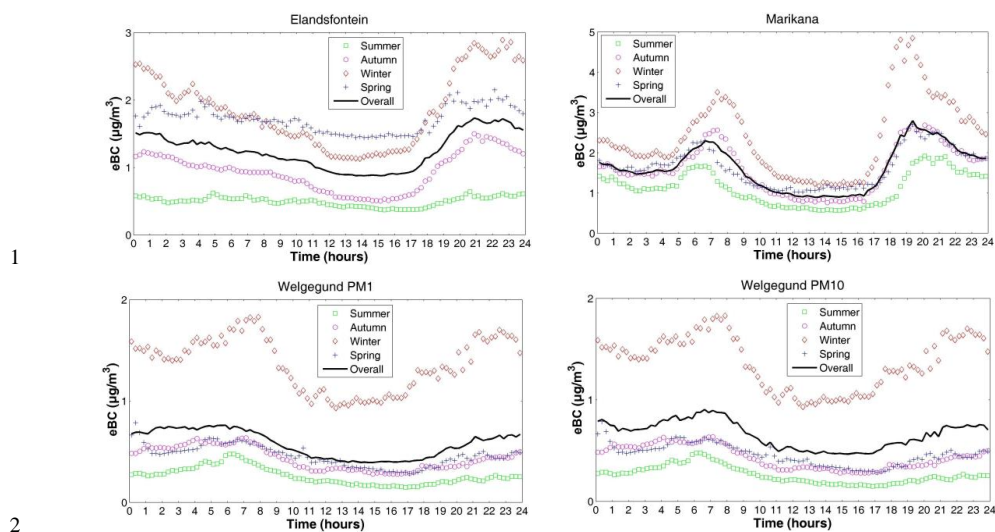4 concentration above the baseline for this example, is also indicated in the top pane.

Atmospheric
Chemistry
and Physics
Discussions

Open Access

Figure 4. Box and whisker plot indicating statistical eBC mass concentrations at the EL, WE and MA sites, as well as EC mass concentrations at the VT, BS, LT, SK and AF sites. The red line of each box indicates the median, the black dot the mean, the top and bottom edges of the box the 25th and 75th percentiles and the whiskers ±2.7σ (99.3% coverage if the data has a normal distribution). The 15-minute a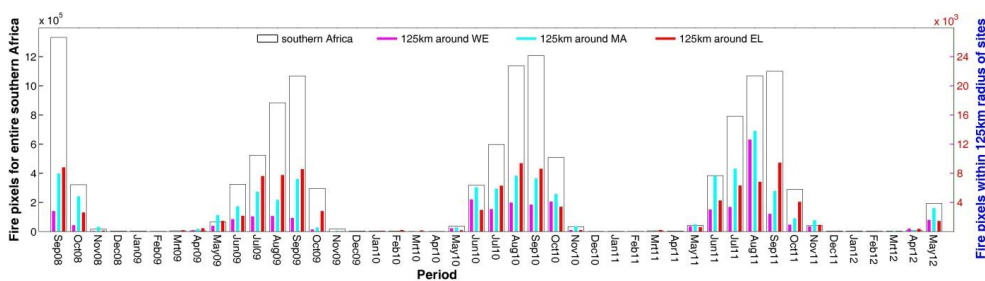nd 24-hour maximum mass concentration values measured at the sites with continuous and off-line analyses, respectively, as well as the number of measurements (N) are indicated.

1

2

3

Figure 5. Monthly statistical distribution of eBC concentrations at the three sites where continuous measurement data were gathered, i.e. Elandsfontein, Welgegund and Marikana. The red line of each box is the median, the black dots indicate the mean, the top and bottom edges of the box are the 25th and 75th percentiles and the whiskers ±2.7σ (99.3% coverage if the data has a normal distribution).
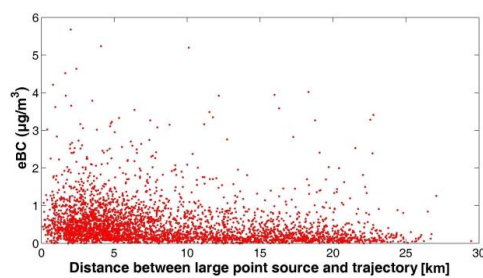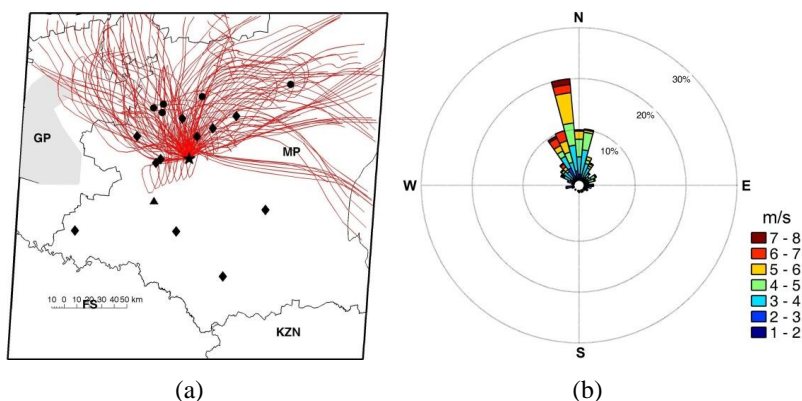
1

2

3   Figure 6.   Overall and seasonal average eBC diurnal patterns observed for Elandsfontein,

4   Welgegund and Marikana. Summer: DJF, Autumn: MAM, Winter: JJA and Spring:

5   SON.

1

2   Figure 7.   Fire pixels within the entire southern Africa (10-35°S and 10-41°E) indicated on the

3   primary y-axis, as well as fires pixels within a radius of 125 km around each

4   measurement site indicated on the secondary y-axis, as determined from MODIS

5   collection 5 burned area product (Roy et al., 2008).

Atmospheric
Chemistry
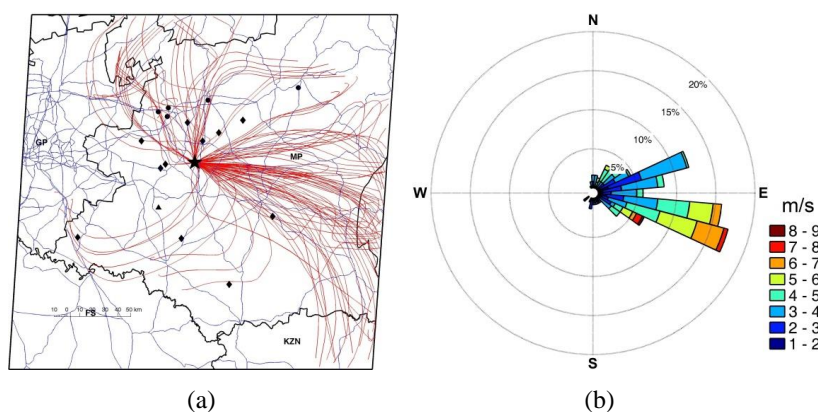and Physics
Discussions

Open Access

1

2   Figure 8.   Hourly average eBC concentrations plotted against the shortest distances that

3   hourly arriving back trajectories passed large point sources during the summer

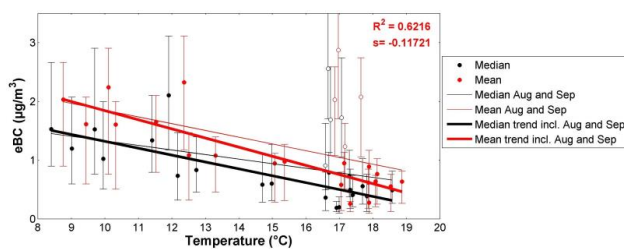4   months, i.e. December to February, at Elandsfontein.

Atmospheric
Chemistry
and Physics
Discussions

1

2   (a)   (b)

3   Figure 9.   (a) All 24-hour back trajectories associated with peaks characterised by coincidental

4   increases in eBC and H$_2$S during December to February. The Elandsfontein site is

5   indicated by the black star. The black dots indicate pyro-metallurgical smelters and

6   char plants, the black diamonds coal-fired power plants and the black triangle a

7   large petrochemical operation. (b) Wind rose showing the prevailing wind direction

8   during periods when eBC plumes that coincided with H$_2$S plumes were observed.
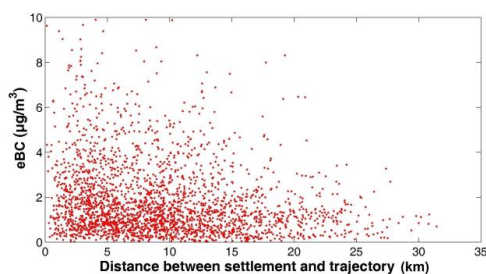
1

2   (a)   (b)

3   Figure 10. (a) All 24-hour back trajectories associated with peaks characterised by coincidental

4   increases in eBC and NO_2 during December to February. The Elandsfontein site is

5   indicated by the black star. The black dots indicate pyro-metallurgical smelters and

6   char plants, the black diamonds indicate coal-fired power plants and the black

7   triangle a large petrochemical operation. Roads are indicated with blue lines. (b)

8   Wind rose showing the prevailing wind direction during periods when eBC plumes

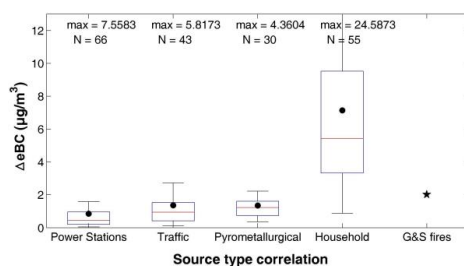9   that coincided with NO_2 plumes were observed.

10

1

2   Figure 11. Monthly median and mean eBC (with bars indicating 25th and 75th percentiles)

3   plotted against monthly median and mean temperatures for Elandsfontein.

Atmospheric
Chemistry
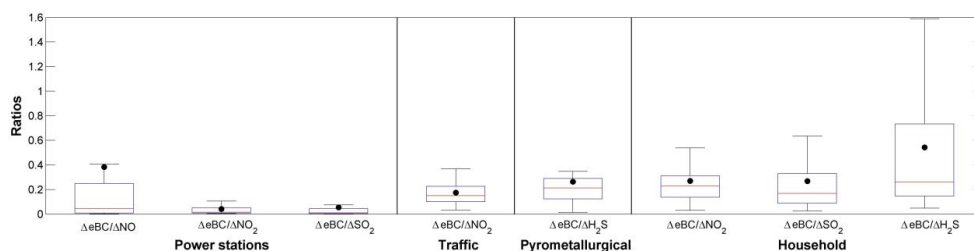and Physics
Discussions

1

2   Figure 12. eBC concentration plotted against the shortest distances that hourly arriving back

3   trajectories passed in- or semi-formal settlements during the winter months of June

4   and July at Elandsfontein.

1

2   (a)   (b)

3 Figure 13. (a) Map indicating 24-hour back trajectories associated with peaks characterised by

4   coincidental increases in eBC with NO_2, SO_2 and H_2S, but not NO in June and July.

5   The Elandsfontein site is indicated by the black star. (b) The wind rose associated

6   with arrival times of plumes associated with household combustion is indicated in

7   Figure (b).

Atmospheric
Chemistry
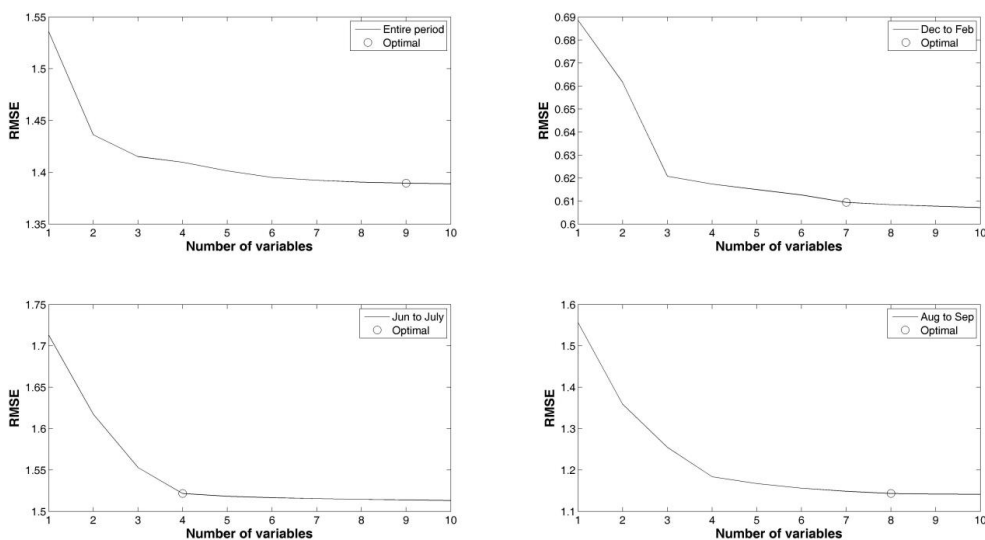and Physics
Discussions
Open Access
EGU

1

2   Figure 14. Δ eBC measured during plumes when eBC increases originated from coal-fired

3   power station, traffic, pyro-metallurgical smelters and household combustion as

4   measured at Elandsfontein. The overall mean baseline increase due to savannah

5   and grassland fires in September is also indicated. This data was normalised to

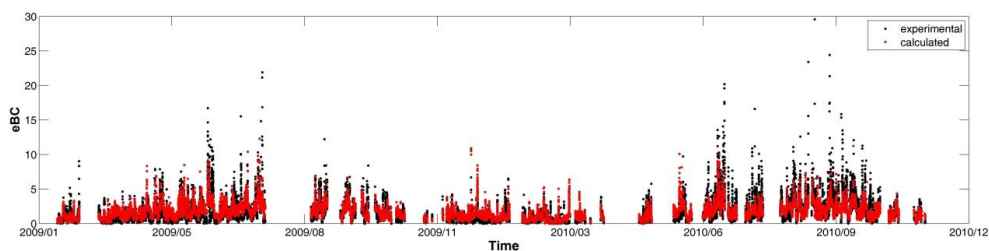6   variations in boundary layer at Elandsfontein (Korhonen et al., 2014).

Atmospheric
Chemistry
and Physics
Discussions

Open Access

EGU

1

Figure 15. Ratio of Δ eBC divided by Δ of other species relevant to the identification of each
source type, except for grassland and savannah fires measured at Elandsfontein.

Atmospheric
Chemistry
and Physics
Discussions

Open Access

EGU

1

2   Figure 16. RMSE difference between the MLR calculated eBC and the actual measured eBC

3   at Elandsfontein for the entire measurement period (top left pane), as well as the

4   December to February (top right pane), June to July (bottom left pane) and August

5   to September (bottom right pane) periods individually.

1

Figure 17. Actual eBC compared with calculated (using Eq. 2) for the entire monitoring period

3   at Elandsfontein.